PROCESS OPTIMIZATION OF A SMALL SCALE BALL MILL FOR MINERAL PROCESSING USING DISCRETE ELEMENT METHOD

PHILBERT MUHAYIMANA

MASTER OF SCIENCE

(Mechanical Engineering)

JOMO KENYATTA UNIVERSITY OF AGRICULTURE AND TECHNOLOGY

2019

Process Optimization of a Small Scale Ball Mill For Mineral Processing using Discrete Element Method

Philbert Muhayimana

A thesis submitted in partial fulfillment for the degree of

Master of Science in Mechanical Engineering in the

Jomo Kenyatta University of Agriculture and Technology

2019

DECLARATION

This thesis is my original work and has not been submitted for examination in any other university

Signature..... Date.....

Philbert Muhayimana

This thesis has been submitted for examination with our approval as the University Supervisors:

Signature..... Date.....

Dr.-Ing. James K Kimotho

JKUAT, Kenya

Signature..... Date.....

Dr.Eng. Hiram M Ndiritu, PhD

JKUAT, Kenya

DEDICATION

This work is dedicated to my mum Rose, my father Raban, my sister Sarah, my brothers, Evode, Richard, Nestor, Robert for being there for me all through my studies.

ACKNOWLEDGEMENTS

My greatest gratitude goes to the Almighty God for His divine protection and guidance throughout my study.

My great thanks goes first to my thesis supervisors Dr.-Ing. James K Kimotho and Dr.Eng. Hiram Ndiritu. The doors to their offices were always open every time I needed assistance and guidance in my research work. Their consistency support allowed this thesis to be my own work. They have directed me in the right direction anytime they thought I needed it.

I would also like to express my pleasure to thank the EU Intra-ACP project titled; "Mobility to Enhance Training of Engineering Graduates in Africa (METEGA) for their financial support to be able to pursuit my studies.

It is also with a great pleasure to thank experts who facilitated my validation work in this research project: Mr Mathew Ndeto, Dadson Mwangi. Without their passionate assistance and advices, the validation of my results could not be conducted.

Finally, I thank my family for their great support and encouragement all through my studies, I would also like to express my profound gratitude to my Co-Mechanical Engineering students for their support through the process of conducting this research. Without their assistance this accomplishment would not have possible. Thank you

TABLE OF CONTENTS

LIST OF TABLES

LIST OF FIGURES

LIST OF APPENDICES

LIST OF SYMBOLS

Symbol	Description
D	Effective diameter of the drum [m]
d_b	Diameter of grinding media particles [mm]
D_m	Mill internal diameter [mm]
E	Net specific energy [J]
F	Charge [t]
Fn_i	Normal force of particle i [N]
Ft_i	Tangential force of particle i [N]
G	Is the Elastic shear modulus [Pa]
H	Is the height of the free space in the mill [m]
h	Distance between the centre and the material in the ball mill [m]
I_i	Moment of inertia of a particle i [$kg - m^2$]
J	Mill filling volume [m^3]
K	Constant for a given material and mill [$constant$]
L	Effective length of the mill [m]
P	Power consumption of the mill at the mill shell [$watt$]
q	Specific charge [%]
S	Specific surface area [mm^2]
S_{max}	Maximum attainable specific surface area [mm^2]
T_i	Torque [Nm]
V	Volume of the mill [m^3]
V_{gm}	Volume of the grinding media inside the mill [m^3]
V_{ma}	Volume of the material inside the mill [m^3]
W	Weight bulk [t/m^3]
w	Work input [kWh/t]
w_i	Work index [kWh/t]
x_f	Feed size [mm]
x_p	Particle size [mm]
α	Angle of displacement [$degree$]
ω	Angular velocity of the drum [r/s]
λ	Friction factor [constant]
ν	Poisson's ratio [constant]

ABSTRACT

A ball mill is a grinding machine widely used in mineral processing to gradually decrease the size of ore particles. It is made of cylindrical drum supported by a frame. The inner part of a grinding mill contains horizontal bar knows as lifters to lift the charge. Ball mills and crusher are classified among comminution machines that consume the most amount of energy in mineral processing industries. A lot of research has been conducted on various parameters that affect the power consumption of ball mill. It has been documented that the power consumption in ball mill usually depends on charge fill level, lifter geometry, and mill speed. In this work, a small scale batch ball mill was modeled and numerically simulated using a 3D DEM software (EDEM). Five types of lifter profiles; rectangular, trapezoidal, triangular, parabolic, and round, were investigated in terms of power consumption and impact load at mill speed ranging between 65-100% of the critical speed. DEM satisfactorily predicted power consumption and impact load for different lifter profiles at different percentages of critical speed. Lifter profiles were found to have average deviation in power consumption of 8.53 Watts as the lifter face angle changes from 0 to 25.56 degrees. This showed a significant impact on the power consumption due to the change in face angle. Lifter number as well as lifter height have shown marginal effect on the power consumption with the change in rotational speed. Rectangular lifters showed higher impact load and lower power consumption compared to other lifter profiles. Sieving analysis demonstrated that mill speed affect the fineness of throughput and 75% of critical speed resulted in the smallest particle size (11% of 150 μm particle passing through) at 209 Watts of power consumption. The lifter profile and its effect on power consumption and impact load finds application in the design and production of small scale ball mill to be used in different mineral processing firms. These include artisanal and small scale miners in Migori, Kakamega, and Narok counties in Kenya, as well as researching institutions. The optimized grinding process plays a great impact in reduction of electricity bills, as well as reduction of fuel consumption for small scale miners, hence requiring optimal lifter profile and effective grinding.

CHAPTER ONE
INTRODUCTION

1.1 Background

In mineral processing, valuable ore is liberated from the gangue in a process known as comminution. This process produces desirable fine grade. Comminution is defined as the size reduction of rock material by the application of energy. Industrial comminution process is estimated to absorb from 3 to 5% of global electric energy consumption (Daniel & Tadeusz, 2010). At a single ore processing plant, comminution accounts for up to 70% of total production costs, either due to equipment maintenance or power consumption.

In mineral processing many comminution machines are used. They differ depending on application and the size. In general, mineral processing machines are classified into two categories; grinders and crushers (B. A. Wills & Napier-munn, 2006). Crushers are used to reduce the size of big ore particles whereas grinders are used to refine particles to a very smallest particles.

Tumbling mill is among the grinder used in mineral processing and works by rotating the ground materials inside the drum. These materials are lifted and dropped, colliding with each other which result into the partcle size reduction. A ball mill is categorized as a tumbling mill and is used in grinding of ore materials to refine particles. It uses balls as grinding media which may be made of steel (chrome steel, stainless steel). A ball mill grinds materials by impact of the grinding balls rotating in a cylindrical shell. The rotation of grinding mill, causes the balls to fall back into the cylinder and onto the materials to be ground. They are used to reduce particle size on a relatively wide range of particle sizes. Hence, their wide application in many industries, production of noncrystalline materials and in research laboratories (Kohta, Hirotoshi, & Etsuo, 2009).

A small scale ball mill is used in mineral processing for artisanal and small-scale mining (ASM). It is a small batch grinding mill used to separate the valuable minerals from the gangue. It comprises of small drum, removable lifters and small gating to remove material when the grinding is over. A power transmission system that reduces the input speed from the motor to a desirable speed of the drum is usually incorporated as shown in Figure 1.1

Small scale ball mills are known to be effective in terms of fine throughput size. How-

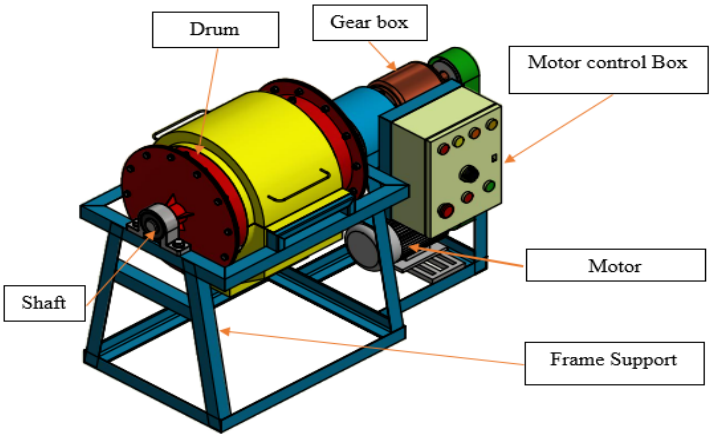

Figure 1.1: Small scale ball mill fabricated at JKUAT

ever the higher power consumption of these grinding machine can be attributed to many different process parameters that lead to huge amount of energy consumption.

(Kyalo, Ndiritu, & Mwangi, 2017) conducted survey in Migori which showed that artisanal miners experience many challenges such as noise, dust, huge power consumption, and low quality of ground materials. To improve the grinding activities of artisanal miners in Kenya, a small scale ball mill was developed at Jomo Kenyatta University of Agriculture and Technology (JKUAT). This ball mill neccessitates optimization in terms of power consumption and structral analysis for effective performance and maintain its integrity and usefulness.

1.2 Problem Statement

Generally, the inefficient ball mill in mineral processing produces dust and noise, and this leads to hazardous conditions, health problems, and low overall performance of the mill (World Health organization, 2016). In addition to that, ball mills are known to use huge amount of wear resistant materials and consume higher energy to provide fine ground materials. All these are affected by different mill parameters such as grinding media and its size distribution, the critical speed of the drum, the mill filling rate, and the liner geometry (Datta, Mishra, & Rajamani, 1999; Nistlaba & Lameck, 2005; Kabezya & Motjotji, 2015; Fuerstenau & Lutch, 1999; Usman, 2015).

A lot of researches have focused on grinding process and performance of a ball mill by considering minimum power consumption and maximum impact load (Austin & Shoji, 1976; Raasch, 1992; Fuerstenau & Lutch, 1999; Karunatilake, Kuhn, & Seibold, 2000; Mio, Saito, & Miyazaki, 2001; Deniz, 2004; Makokha & Moys, 2006; Kiangi & Moys,

2008; Prasad & Theuerkauf, 2010; Soleymani, Fooladi, & Rezaeizadeh, 2017; Yin, Peng, Zhu, Yu, & Li, 2017). This include studying the motion of ball charge, and power consumption using DEM (Mishra & Rajamani, 1992), the study of the effect of mill speed on the charge behavior, torque, and power consumption(Cleary & Hoyer, 2000). All these studies contributed to the evolution of large scale ball mill development. However, small scale and large scale ball mills differ in efficiency, size, shape and material to be ground, whereby large scale ball mills are more efficient than small scale ball mill. Therefore the lifting action of charge materials in small scale ball mills necessitates further research. First, the DEM utilized for optimizing the lifter geometry only focused on industrial grinding mills. Second, the grinding process for small scale ball mills requires to be favorably validated using small scale trials rather than plant trials. It is therefore necessary to evaluate the influence of different geometries of lifters (lifter profile, lifter number, lifter height), and mill speed, on the power consumption and impact load of small-scale ball mill.

1.3 Objectives

The general objective was to optimize process parameters for a small scale ball mill so as to reduce power consumption and offer effective grinding. This would be done through simulation using discrete element method. The main objective was achieved through the following specific objectives.

1. Development of a geometrical model for a small scale ball mill to study the grinding process.
2. Evaluation of the effect of lifter geometry, and mill speed as well as optimization of the power consumption and impact load of a small-scale batch grinding mill through simulations using EDEM software.
3. Experimental investigation of the effectiveness of grinding of the ball mill with respect to fineness of throughput materials in order to validate the simulation results.

1.4 Justification

A grinding mill uses much energy to reduce the size of ground materials to micro-size of granular materials; that is the throughput of the system. In addition to most energy usage in operation, they also require a large number of wear resistant materials, which are utilized for mill liners and grinding balls.

Researchers have considered different parameters as mentioned above, but with little at-

tention on the effect of the geometry of lifters on the overall performance of grinding machine.

The (U.S Department of energy, 2007), showed that the total milling cost (energy, grinding media, lifters, and labor cost) is affected by the mill lifter particularly in autogenous (AG) and semi-autogenous (SAG). Later (Royston, 2008), added that the prime purpose of lifter design is to increase the falling rate of grinding media at the toe of charge, to prevent lifter and ball from damage, and to improve the economics related to liner wear life. (Dahner & Bosch, 2011) showed in Figure 1.2, how a non-optimized liner/lifter design influence the total milling cost. Even though the cost of non-optimized liner 9.6% of the milling cost it influences the media and energy cost whereas the optimized lifter cost is 13% and it saves 26% of the total milling cost. This emplies that the optimized liner is expensive and contribute to the reduction of the total milling cost whereas the non-optimized liner is cheap and infulances other parameters cost.

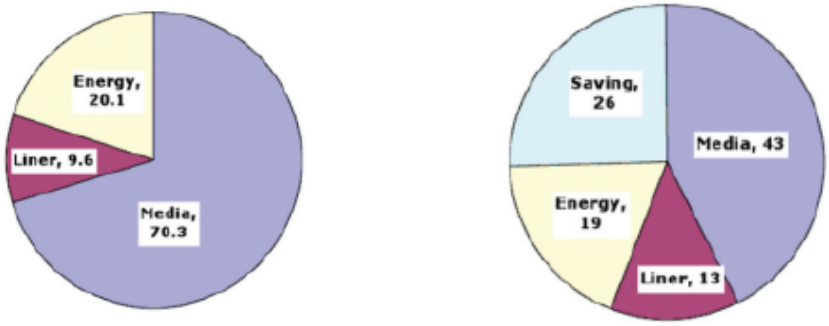

(a) Non-optimizedlifter design cost (b) Optimized lifter design cost

Figure 1.2: Milling cost of optimized and non-optimized liner design

The optimal mill liner is expected to provide more efficient grinding media by maximizing media drop height and maximize impact load of grinding balls. This would promote efficient grinding media trajectories, resulting in effective grinding and maximize mill throughput desired size, and reduce the energy more efficiently.

1.5 Outline of the Thesis

This thesis is divided into five chapters. The present chapter is the introduction which contains the background of this work, main definitions, problem definition and objectives of this research. Chapter 2 covers the relevant researches concerned with parameters that

affect the power consumption and impact load of ball mills. Chapter 3 covers the theory behind the proposed models, it contains governing equations, and methodology used to analyze the power consumption and impact load of small scale ball mill. Chapter 4 presents results based on DEM simulations. Conclusion and recommendation drawn in this research are presented in chapter 5 together with further research to be carried out for having optimal grinding mills.

CHAPTER TWO
LITERATURE REVIEW

2.1 Introduction

This chapter, presents a review of what has been done by many researchers. The attempts of many researchers to optimize the process parameters of a ball mill. A general review of DEM is presented, and the effects of operational parameters on the performance of a ball mill in comminution.

2.2 Concepts of Comminution and Equipment

2.2.1 Comminution

Comminution is defined as size reduction process which involve breaking-down of bulk solid materials into smaller particles, without altering their state of aggregation (Daniel & Tadeusz, 2010). Comminution comprises of three steps: rock blasting, crushing, and grinding. Each one of the three stages has a particular comminution machine.

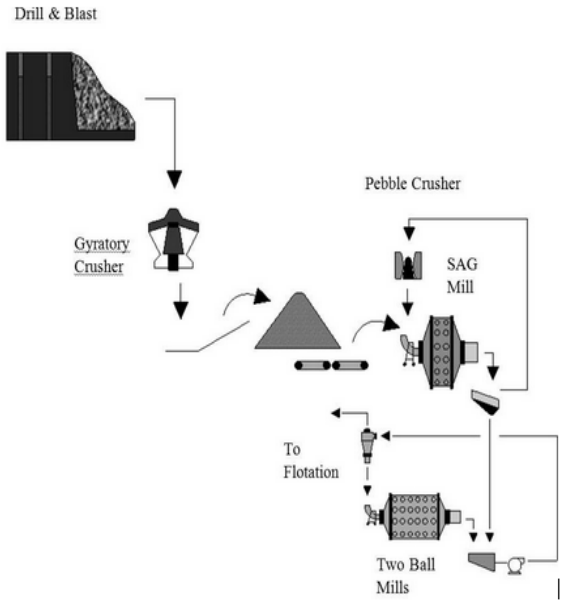

Figure 2.1: Comminution process in mining industry (Nadolski et al., 2014)

Figure 2.1, illustrates the comminution process in mining industry. The rock is blasted and big stones are fed in primary crushers also known as gyratory crushers. The stones are reduced in size and are fed in secondary crushers also known as jaw crusher. The

size of the stones is reduced further and are finally fed in ball mill to provide very fine particles.

Rock blasting consists of drilling holes in the rock walls or benches. The holes are filled with chemical explosive to explode the rock and cause cracks to propagate in the rock. The explosion releases multiple fragments of the rock which are suitable for crushing.

Crushing follows rock blasting. It is in this process that big blasted rocks are reduced to achieve the desired size for grinding. Crushing of rocks is normally done by use of stone crusher machines. Crushed ore from the crushing circuit is fed to the grinding machine to produce particles that are liberated from the gangue. The particle are small enough and consist mostly of one mineral.

Grinding is a process of reducing the rock material to very small particles using a mill. Grinding mechanism of ball mills consist of cylindrical mills rotating about the horizontal axis. The mill drum is usually filled partially with charge materials which may consist of grinding media, ground materials also known as ore particles and sometimes water. The motion of charge materials and their interaction inside the mill depends on the applied energy and the mill geometry (liner type, lifters profile and mill diameter). Lifters are used to avoid slipping of granular materials and to reduce the amount of energy used within the grinding process and therefore improve the breakage of particles by increasing the number of collisions and impact load. Hence the dimensions of the lifters and their configurations have great influence in charge motion and grinding efficiency (Francioli, 2015).

2.2.2 Ball Mill

Ball mills are used in many applications and can vary in size from small scale batch ball mills up to huge autogenous mills with outputs of hundreds tons per hour depending on the application. Small scale ball mills are used for batch grinding in mineral processing on small scale to grind granular materials and liberate them from the gangue to achieve a very fine throughput.

Ball mills are said to be advantageous because they provide very fine particles which are less than 10 microns, they are also good for continuous application and widely used in milling highly abrasive materials due to the fineness of throughput. They also have disadvantages such as: high machine noise level especially when the drum is made of

metal, relatively long time of milling and high power consumption (Cleary & Morrison, 2011a).

The rotating motions of balls in ball mills are classified in three distinct regimes of rotation speed: Centrifugal, Cascade, and Cataract. Ball mills are known to operate in two distinct regimes of rotating speed: cascade and cataract, as shown in Figure 2.2(a), (b). Cataract is more likely to favor collisions and body breakage whereas cascade motion would result in breakage through attrition. Centrifugal is defined when the mill drum is rotating at a very high speed that results to the grinding media to move adjacent to mill shell known as critical speed. In this regime ball mill can not grind, the grinding balls are not falling for impact as shown in Figure 2.2(c).

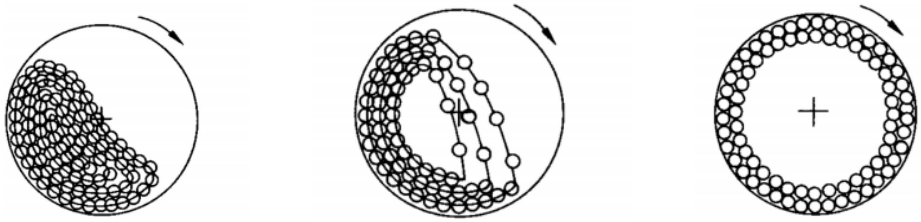

(a) Cascade (b) Catract (c) Centrifugal

Figure 2.2: Distinct regimes of rotation speed of a ball mill (Balaz, 2008)

Grinding mills should operate at an operational speed below critical speed (Michael, 1988). Critical speed is the speed at which centrifugal forces equal gravitational forces at the mill drum's inside surface. At this speed, the balls will not fall unto the toe wich is the point of contact at the mill wall. When the drum is rotating at a very high speed, balls are moving adjacent to the mill shell hence there is no impact of the grinding media to the rock materials.

The most common reasons for grinding of particles are to; create appropriate particle sizes, improve material mixture, prevent segregation, increase the material's surface area, control a material's bulk density, liberate impurities, reduce porosity of the particles, and modify the shapes of particles(Tang & Puri, 2004).

The charge motion has been described to have different regions inside the rotating ball mill as illustrated in Figure 2.3 by (Powell & Mcbride, 2004). In this illustration the shoulder was defined as the upper most point at which the charges will depart from the mill shell. Toe is the point at which the cascading particles collide against the mill shell.

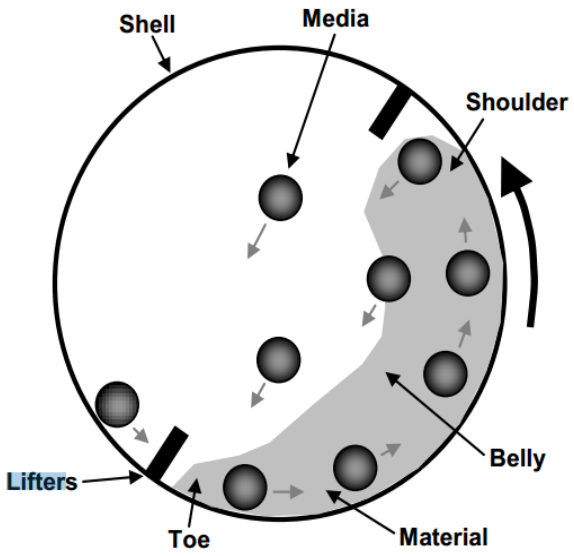

Figure 2.3: Main feature of the charge motion inside a rotating ball mill (Powell & Mcbride, 2004)

2.3 Comminution Process

Comminution machines have been used many years back, and by the end of 19th century (Lynch & Rowland, 2015), the need for a grinding mill that can produce finer particles had become a problem. The existing mills driven by steam engines had limitations on how they could grind and provide better fine particles. At that time, cement production was very necessary and had to be ground very fine to make appropriate cement. However, technologies they had were not effective and had high maintenance cost. Inventors focused on making a fine-grinding machines, and tumbling mills were developed.

The tumbling mills consist of a horizontal cylinder that contain charges; grinding media and particles to be ground. They rotate at a horizontal axis, the material inside the cylinder are lifted up by the liner and fall back unto the toe. The invention of tumbling made it possible to produce finer particles in micrometers. Tumbling mills were subdivided into many categories depending on the application, size, and the type of grinding media. Ball mills, use steel balls and are mostly used for finer grinding. Although, the problem of getting finer particles were solved by the development of tumbling mills, the energy consumed during the grinding process was still a problem.

(Rittinger, 1867) developed a theory known as *The First Law of Comminution*, which states that the energy consumption is proportional to the increase of surface area generated

by crushing or grinding processes. It is known that surface area is inversely proportional to particle size, resulting in the following equation:

$$E = K\left(\frac{1}{x_p} - \frac{1}{x_f}\right), \tag{2.1}$$

where x_f and x_p are feed and product particle size respectively, K is a constant for a given material and mill and E is the net specific energy required (Lynch & Rowland, 2015). The coefficient K depends on the shape of the particle, the type of material, the number of defects and the efficiency of the forces applied for the comminution work. However, the law that was developed ignored the energy absorbed by elastic deformation which is several times greater than that required for creation of new surfaces.

(Tanaka, 1966) summarized the work of Kick, Bond, and Hukki. He showed that Kick developed another theory known as *The Second Law of Comminution*. It assumes that the energy consumed is proportional to the volume reduction of the particles involved and it can be given by:

$$E = K\ln\left(\frac{x_f}{x_p}\right), \tag{2.2}$$

where x_f and x_p are feed and product particle size respectively, K is the coefficient of materials properties (Tanaka, 1966). The main limitation of this theory was that the energy required to reduce 10 μm particle to 1 μm was the same as the energy required to reduce 1 m boulders to 10 cm blocks (Rhodes, 2008).

(Bond, 1968) developed another theory known as *Third Law of Comminution* which states that, the energy required to reduce particles is directly proportional to the reduction ratio of feed particle diameter to product particle diameter. Bond's theory held that the work varies inversely as the square root of the product particle diameters. In other words the energy consumed to reduce particle size is proportional to the square root of the new area produced and inversely proportional to particle size, and is given by:

$$E = K\left(\frac{1}{\sqrt{x_p}} - \frac{1}{\sqrt{x_f}}\right) \tag{2.3}$$

where x_f and x_p are the feed and product size indices, respectively, K is a constant equivalent to $10W_i$, (where W_i is the work index) and E is the net specific energy. The work index

W_i which was proposed by Bond is determined experimentally in the laboratory. It can be noted that all the developed theories had common limitation, they do not consider particle size distribution of the feed and the product, particle interactions, the energy consumed by plastic deformation (Jankovic, Dundar, & Mehta, 2010).

Hukki revised these energy-size relationships stating that each of Rittinger, Kick and Bond theories might be applied for different narrow size ranges (Tanaka, 1966). Kick's equation is valid for crushing, Rittinger's equation is applicable for finer grinding, and Bond's equation can be used in the conventional milling range. Hukki suggested that Equation 2.4 can be used as a general form of comminution.

$$dE = -K\left(\frac{d_x}{x^n}\right) \tag{2.4}$$

where d_x is the variation in dimension that needs a work dE per unit of volume. The exponent n is not constant; it depends on the characteristic dimension of the particle therefore the revised energy-size equation has the following form:

$$dE = -K\left(\frac{d_x}{x^{f(x)}}\right) \tag{2.5}$$

(Jankovic et al., 2010), concluded that the application of Kick's and Rittinger's theories, though has been met with varied success, they are not realistic for designing size reduction circuits.

New experimental approach using X-ray photograph to measure strain of particles was developed, however, it was still difficult to determine the stress induced in a particle sample. (Dantu, 1957), developed a testing technique to determine contact forces between particles. The technique suggested the use of optically sensitive particles. The method achieved the measurement of contact force and displacement of rotating particles inside the rotating cylinder, but the analysis was time-consuming.

Later, (Cundall & Strack, 1979) developed a numerical method known as discrete element method capable of handling particles of any shape and their interaction for analysis of the rock mechanics problems.

2.4 The Discrete Element Method

Discrete element method is a numerical modeling technique that allows the description of mechanical behavior of interacting distinct materials through contact laws. This method is generally unique due to its inclusion of rotational degrees of freedom as well as stateful contact and often complicated geometries including polyhedra. DEM uses two simple theories: **Newton's Second Law** and **Force Displacement Law**. The force displacement law calculates forces at the contacts between particles, and then the effect of these forces on each particle is determined from Newton's Second Law (Cundall & Strack, 1979). The update of the position of each particle are then used to calculate the new contact forces and this cycle is repeated for each time step. Thus these two contact laws are used in simulations to indicate the movement of the particles in the ball mill (Sullivan, 2008). This process is summarized in Figure 2.4.

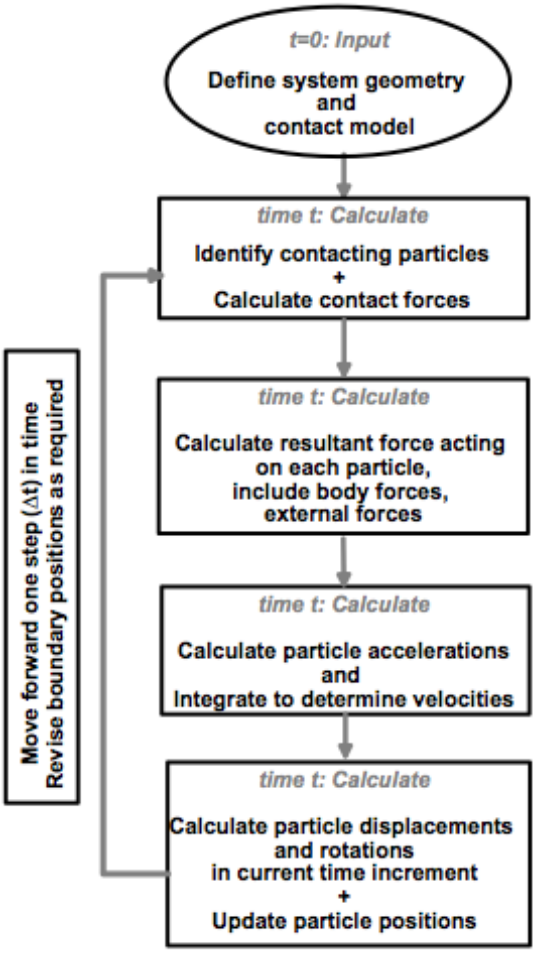

Figure 2.4: DEM Calculation Cycle (Sullivan, 2008)

2.5 Numerical Simulation.

Discrete element method (DEM) is a numerical technique used to model interaction between individual particles and boundaries for predicting bulk solids behavior. This method can easily model moving boundaries and to gain better insight on particle flow dynamics. The knowledge is therefore applied to design more efficient equipment, thus optimizing process efficiency and product quality. This section presents the methodology employed to carry out the DEM simulations.

In DEM method, ball motion and their interaction are based on an iterative process in which the results in each time-step are based on the previous results due to the repetition of the same algorithm in every time-step. A finite number of sphere particles interact with each other, and two iterations are calculated in each time step:

1. Contacting forces are generated based on the overlaps between particles.
2. Movement of particles are updated based on previous movement information and current contact forces.

In the first step, the contact forces between neighbor particles are the dominant factor of resultant force changes, thus the Force-Displacement law plays an important role. For each time-step, the contact forces are changed. In the second step, Newton's second law evaluate how the contacting force determines the movement. Taking one particle in one time-step for instance, the resultant force on a particle would be regarded as the same during this time-step; the current acceleration of the particle would be estimated by resultant force divided by mass, and the new velocity and position of this particle are obtained based on the previous position, velocity plus the integration of the current acceleration over the time-step. This is called the Law of Movement.

As it can be seen, the above description only considers one particle; the DEM method would go through the whole system to update their movement for each and every particle and the new contacting forces for all contacts for every time step.

In the DEM simulations the interaction between two particles is guided by the following equations:

$$F = m\ddot{x} \tag{2.6}$$

$$F = K_n U_n \tag{2.7}$$

where m is the particle mass, $\ddot{x}$ is the acceleration, F is the contact force, K_n is the stiffness for elastic material, U_n is the overlap between particles. The first equation is the Newton's second law, and the second equation means that the contact model between particles is a linear elastic model. Thus, DEM is composed of two parts: law of motion and force displacement law as it can be seen in the Figure2.5 below

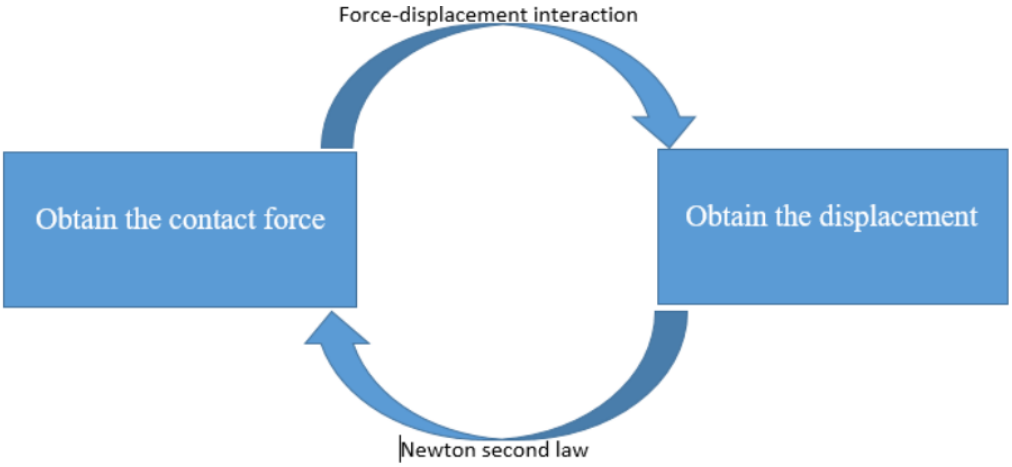

Figure 2.5: Flow chart of DEM principle

2.5.1 Law of Motion

Law of motion is based on the Newton Second's law. In a particulate system, a single particle is affected by 3 types of forces: gravity, normal force, tangential forces and its motion can be described by Equation 2.8

2.5.2 Force-Displacement Principle

The force-displacement principles describe the relationship between relative movement of two particles and the contacting force. The relative motion can be described as two independent parts: normal direction and tangential direction. The direction of normal contacting displacement is always pointing from the center of one entity to that of another, and the 'displacement' factor in this displacement force principle is designated by effective overlaps. There are two types of contacts: ball-ball contact and ball-wall contact. The effective overlap in ball-ball contact is the overlap length in the line that connects two balls' centers. For ball-wall contact, the effective overlap is equal to the radius of sphere

minus the shortest distance from the center of ball to the wall.

(Cundall & Strack, 1979) were the first to use discrete element method, the method was based on the use of an explicit numerical scheme in which the interaction of the particles materials can be traced contact by contact and the motion of each particle can be modeled. Since then, DEM has been adapted to suit many other applications such as, granular flow, powder mixing, and in modeling of many physical systems. (Lorig, Brady, & Cundall, 1986), analyzed the rock-support interaction using DEM, (Campbell & Brennen, 1985), used DEM for granular shear flow analysis, (John M.Ting, 1988), used DEM based on two shaped element to model granular soil behavior, (Mishra & Rajamani, 1992), simulated the behavior of balls in a milling machine using DEM, (Raasch, 1992), analyzed the motion and impact velocities of grinding bodies in planetary ball mill, (Datta et al., 1999) analyzed the power consumption in ball mills using discrete element method, (Kim & Choi, 2008) analyzed ball trajectories to evaluate the grinding mechanism of a stirred ball mill with 3D DEM model.

In DEM particles are usually modeled either in two dimensional (circular discs) or three dimensional (spherical). However, the particles shape can also be modeled in another shape such as ellipsoid (M.Ting, 1992), and polygon (Ghaboussi & Barbosa, 1990), as well as irregular shape which can be modeled by bonding several spherical or circular particles (DEM Solutions, 2011). Many publications on modeling and simulation of grinding mills have used DEM, many of them were limited in 2 dimension (2D) model. (Hlungwani, Rikhotso, Dong, & Moys, 2003) used a 2D model laboratory scale to validate the DEM modeling of liner profile and mill speed effects. (Cleary, 2001) also used a 2D DEM model to establish the charge behavior and power consumed by a 5 m diameter ball mill, relating them to the operating conditions, charge composition, and liner geometry. (Djordjevic, Shi, & Morrison, 2004) have shown that 3D DEM simulations give more accurate results than 2D DEM simulations.

The DEM modeling that is used by (Datta et al., 1999; Mishra & Rajamani, 1992) involves determining the particles that are in contact, the amount of overlap and related velocities. Therefore the net forces acting on the contacting force can be obtained. Newton's second law of motion is used to all particles to determine new particle positions, their velocities and acceleration.

The particle motion in ball mill is based on the Newton second's law of motion. In a

particulate system, a single particle is affected by 3 types of forces: normal force, gravity, tangential forces and its motion can be described as :

$$m_i \frac{dv_i}{dt} = \sum F_{n,i} + F_{t,i} + g, \tag{2.8}$$

$$I_i \frac{d\omega_i}{dt} = \sum T_i, \tag{2.9}$$

The subscripts i is for representing particle, m is the mass of particle, v is the velocity of the mass center, ω the angular velocity, $F_{n,i}$, the normal force of particle i, $F_{t,i}$ the tangential force of particle i and T_i is torque. In these equations m_i and I_i refers to the mass and moment of inertia of a particle i and $v_i = (v_{i,x}, v_{i,y}, v_{i,z})$ and $\omega_i = (\omega_{i,x}, \omega_{i,x}, \omega_{i,x})$ are their linear and angular velocity components. Considering the time step, the movement of a particle will be described by five factors: its position x, velocity $\dot{x}$, acceleration $\ddot{x}$, angular velocity ω, angular acceleration $\dot{\omega}$. They are all determined by resultant moment and the resultant force.

2.6 Contact Model

There are two main categories of contact interactions: particle-to-particle and particle-to-geometry, and have both been used in this research. These interactions are mostly used for simulating different materials. Particle-to-particle contact models, can be classified as contacting force and non-contacting force models. Generally four types of contact models are known to be: continuous potential model, elastic model, visco-elastic, and plastic model respectively. The first one belongs to non-contacting force model, whereas the other three belong to the contacting force model. The continuous potential model is mostly used in molecular systems, and includes Van der Waals forces, electrostatic forces, and liquid bridge forces. The elastic model can be sub-classified as linear elastic and nonlinear elastic model (Peng, 2014).

In DEM, a collision can be either particle to particle or particle to geometry, and is represented by the contact model which show how the colliding bodies interact. Numerous contact models have been used to model the interaction of different particles. The linear spring-and-dashpot used by (Cundall & Strack, 1979), (Morrison & Cleary, 2004), and (Datta et al., 1999); the modified linear viscous damping model (Powell &

Mcbride, 2004), the bi-linear(Powell & Mcbride, 2004); Hertz-Mindlin non-linear spring-and-dashpot,(DEM Solutions, 2011; Fuerstenau & Lutch, 1999). Among all the contact model two models are commonly used.

1. Linear spring contact model
2. Hertz mindlin contact model

2.6.1 Linear-Spring Contact Model

In this model, the displacement is assumed to be directly proportional to the force and it is based on the work of (Cundall & Strack, 1979). Figure 2.6, illustrates the decomposition of collision force into normal and tangential forces with separated by the spring-dashpot elements. For each component, a spring and dashpot is defined to calculate the force. The coefficient of friction is used to control the transition between a sticking and sliding collision, and it poses an upper limit to the tangential force. It is required now to determine the characteristic impact or overlap velocity as an input parameter (Kulya, 2008).

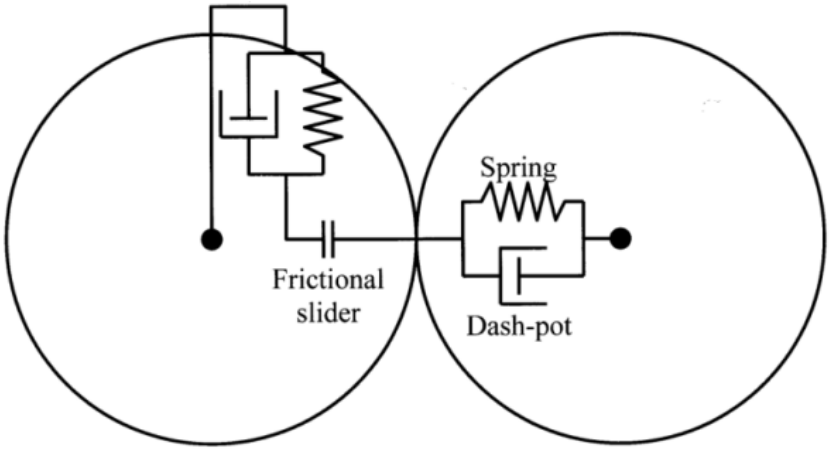

Figure 2.6: Linear-spring contact model(Navarro & de Souza Braun, 2013)

In linear spring-and-dashpot contact model, the contact force in normal direction F_n can be governed by

$$F_n = -b_n V_n + k_n U_n, \tag{2.10}$$

where b_n, U_n, k_n, V_n are; the normal damping constant, the overlap of contacting particles, the normal contact stiffness, and the relative normal velocity of particles respectively.

The linear spring-and-dashpot model is widely used, especially in modeling particles in

fluid, but for dry grinding, it has one major problem. It is contrally to the law of physics as a model for particle collisions. In this model the viscous damping is assumed to be maximum as the particles are coming into contact and also as the particles are about to separate. Damping should be a minimum when the particles first come into contact and also as the particles rebound. Due to the rather unphysical nature of the linear spring-and-dashpot model hypothesized by (R. Sarracino, A. McBride & Powell, 2004) may be adequate for charge motion and power consumption predictions, but it would not generate accurate impact energy spectrum predictions.

2.6.2 Hertz-Mindlin Contact Model

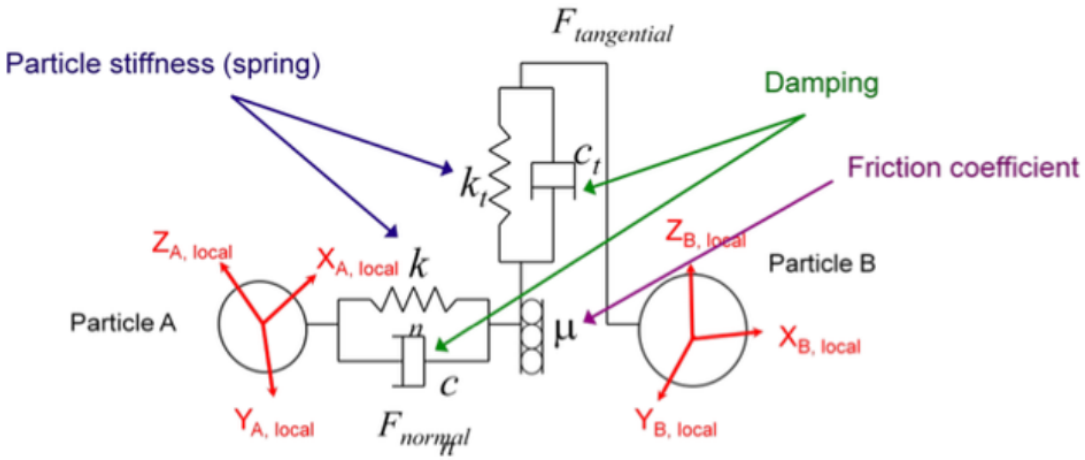

Figure 2.7: Hertz-Mindlin model (Härtl & Ooi, 2008)

Figure 2.7, illustrates the Hertz-Mindlin model which is widely used in EDEM simulations (DEM Solutions, 2011). It uses two spring-dashpot responses. One for normal contact between particle to particle and/or particle to geometry which has a Coulomb friction coefficient μ for shear interactions. The second for response to tangential or rolling friction interaction. It provides an alternative, to the more common linear spring-and-dashpot modeling and illustrates more detailed and realistic interaction between the two particles A and B than the spring-and-dashpot model (Jaeger, 2005). Unlike the linear contact model, in the Hertz-Mindlin contact model, the normal spring stiffness, k_n, varies according to the amount of overlap, U_n, between the contacting particles. It is in accordance with Hertzian contact theory developed by reviewed by (Johnson, 1985). The total contact force can be subdivided into two forces: normal and tangential forces. Spring and

damping components are used for the two forces, friction for only tangential component, and coefficient of restitution for the normal force component. This model calculates the normal and tangential forces using material properties such as the coefficient of restitution, Young's modulus, Poisson's ratio, size and mass. This model is a non-linear elastic model; thus it is well suited to the non-cohesive interactions which are to be used within the computational models (Härtl & Ooi, 2008).

Using Hertz-Mindlin contact model, the interaction of particles is governed by the Hertz theory;

$$F_n = 2/3 P_{max} \pi a^2, \tag{2.11}$$

where P_{max} is the maximum pressure at the point of contact, and a is the area covered by the contacting bodies.

$$a = \frac{3 P_{max} R^*}{4 E^*}, \tag{2.12}$$

R^* and E^* are the reduced radius of contacting bodies and young modulus respectively. Hence the force- displacement relation in the normal direction is calculated by

$$F_n = -k_n {U_n}^{3/2}, \tag{2.13}$$

U_n is the contact overlap and k_n is the normal contact stiffness.

2.7 Contact Model Parameters

Material properties and material interaction parameters, such as: the spring stiffness or Young's modulus and poisson's ratio, damping constant or coefficient of restitution, and coefficient of friction are required in the early discussed contact models. (Chandramohan & Powell, 2005) said that instead of using estimate and approximate values of material interaction properties, they can rather be measured to provide an overall reliable and accurate result in predicting the motion of grinding media in ball mill.

2.7.1 Coefficient of Restitution

The damping constant and coefficient of restitution are important interaction parameters for the prediction of charge motion and energy distribution of particles inside the rotating mill. They represent measures of the energy that is lost during a collision. The coefficient of restitution is defined as the ratio of the relative velocities of colliding bodies just before contact, to the relative velocities just after the collision (Johnson, 1985).

2.7.2 Contact Stiffness, Young's Modulus and Poisson's Ratio

The resultant force from the overlap at the point of contact is a function of the contact stiffness. The selection of this parameter is necessary in DEM measurement. In Hertz-Mindlin model, the stiffness k is known as a function of young's modulus E and Poisson's ration ν which are related such that;

$$E = 2(1+\nu)G, \tag{2.14}$$

where G is the elastic shear modulus which is mostly used in DEM simulations.

2.7.3 Coefficients of Static Friction

The coefficient of static friction is defined as the friction force between two particles when neither of the particle is moving. The coefficient of kinetic friction is the force between two objects when one object is moving, or if two particles are moving against one another. The coefficient of friction governs the initialization of slip between two particles experiencing tangential interaction. (Van Nierop, Glover, Hinde, & Moys, 2001) reported the variation of the power draw with coefficient of friction, and suggested that the coefficient of friction may be an important parameter in DEM simulations.

2.8 EDEM Software

EDEM is used as a powerful tool with the capacity of post processing data. It allows the extraction of any type of information used during the simulation stage. However, the more it generates data, the more the computational power, which leads to several gigabytes in some cases (de Carvalho, 2013).

DEM simulations of grinding mills started as a 2-D dimensions technique: Millsoft, and was improved to 3-D softwares, such as EDEM, which came out with the advances in computational power. Recently, DEM tools have been improved to be coupled with other simulation techniques, for instance: DEM-FEM (Finite element method), DEM-CFD (Computational Fluid Dynamics) and DEM-SPH (smoothed particles hydrodynamics)(Peng, 2014).

Simulation results requires validation. DEM results have to be compared with experimental results. Validation is necessary to check how closely the model's prediction agrees with the observed reality. (Cleary & Hoyer, 2000) conducted an experiment using a centrifugal

mill and changed fill levels. Their experimental data was found to be in good agreement in terms of power prediction.

(Makokha, Moys, Bwalya, & Kimera, 2007) carried out another study to compare simulations data and experimental data by using a ball mill with different lifter profiles. The obtained results were with good agreement regarding the shoulder and toe positions as well as power consumption at a wide range of critical speeds. (Djordjevic et al., 2004), conducted an experiment using a pilot AG mill. It was observed that the error in power consumption predicted using DEM was 3.1%.

Variation of the methods used in DEM generally depends on the inclusion of rotational degrees-of-freedom as well as stateful contact and often complicated geometries (including polyhedral). Today, DEM has become a widely accepted tool to effectively address engineering problems in mineral processing and discontinuous materials, especially in granular flows, powder mechanics, and rock mechanics. Recently, the method was expanded into the Experts in Discrete Element Method (EDEM) taking into consideration the coupling of thermodynamics, fluid dynamics, and finite element method tools (Börner, 2011). EDEM consist of the following main components as shown in Figure 2.8:

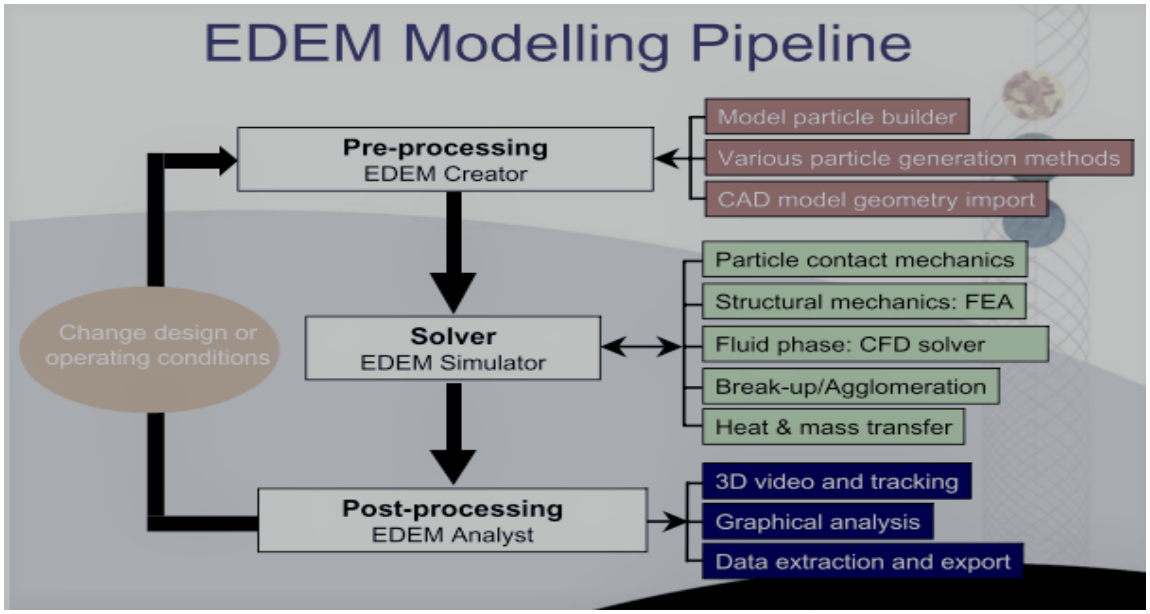

Figure 2.8: EDEM software flowchart(Sergio et al., 2013)

I EDEM Creator

In this section of EDEM, simulation inputs are set and the boundary conditions entered. Material properties and their interactions have to be defined. The coefficient of restitution, coefficient of static friction and rolling friction are entered. The geometry model and particles to be used in simulation are imported and their material properties are defined. Finally, a factory to generate particle is selected among the two particle factories (Static, and dynamic factories) (DEM Solutions, 2011).

II EDEM Simulator

In this section, the simulation created in EDEM creator is ready to run. Important input parameters are entered mainly the time step, the data save interval and the total simulation time. The time step is incredibly important for producing accurate results. Even though small time steps increases the total computation time, it also increases the accuracy of the model. The data save interval defines how often the data will be stored, and so is very important to the analysis (DEM Solutions, 2011).

2.9 Parameters that Affect Grinding Mechanism of Ball Mills

In mineral grinding using ball mills, there are factors that have been investigated and applied in ball milling industries in order to maximize grinding efficiency (Francioli, 2015).

2.9.1 Mill Diameter

The mill diameter is among parameters that affect the performance of ball mills. Researchers have investigated mill diameter. (Bond, 1968) observed grinding efficiency as a function of ball mill diameter and established empirical formulas for recommended media and mill speed that take this factor into account. The mill diameter determines the operating speed of a grinding mill (King, 2000; Deniz, 2004).

(V. Gupta, Zouit, & Hodouin, 1985) used the population balance model to investigate the effect of ball and mill diameters on grinding rate parameters when grinding quartz, the ball diameter has a range of 1.27 to 3.81 cm. The particle size was $8/10$ to $100/150$ mesh. A new correlation has been developed to describe the effect of ball and mill diameters on the rate parameters, concluded that grinding rate parameters vary with ball and mill diameters.

(Rowland, 2006) also conducted a study and predicted the power consumed and charge motion for different mills diameter with the same lifter shapes run at the same operating conditions. 50% ball load was selected. It was observed that different mill diameters can draw different power around this load. Power consumption for small scale to large scale mills was then predicted using the DEM simulations. It was observed that as mill diameter increases, simply the power consumption of the mill also increases. In the foregoing studies a mill diameter, the number of lifters that can be fitted in one specific mill diameter were not investigated.

2.9.2 Mill Speed

When designing a ball mill, much consideration is needed on the size of the drum of ball mill and its operational speed. It has been shown in the publications of (King, 2000; Deniz, 2004) that the mill diameter and mill speed have a great impact on the grinding process of granular material .

(Deniz, 2004) investigated the effect of mill speed on the limestone and the clinker samples at batch grinding conditions based on a kinetic model. The effect of operational speed which is the fractional to critical speed Cr on the grinding for model parameter was found to be different for two different samples. It was found that, for batch grinding, optimum grinding occurs at operational speed $\phi_c = 85\%$ of the critical speed.

(Francioli, 2015) conducted another study on the effect of different operational variables on ball milling. The effect of mill filling, powder filling, percentage of critical speed, ball size and percentage of solids, were evaluated. The selection of the grinding media of was 25 mm, 30% mill filling, 100% powder filling and 75% of the critical speed was selected to be the the base condition. All other subsquent tests were varied according to the progress of the results and the need to evaluate tests with different operational variable. In the study, the critical speed was taken as the reference speed and concluded that the effective operating rotation of a mill is within two distinct regimes depending on the rotation speed: cascade and cataract, as illustrated in Figure 2.2. The cascading motion resulted in breakage through attrition whereas the cataracting motion would favor collision impact and, thus, body breakage. Figure 2.9, illustrates the variation of power with respect to mill speed. It shows that the power consumption increased with the mill speed due to the dislocation of the center of mass of the charge towards the mill shell. However, when the mill speed increase further toward the critical speed the center of mass is dislocated

to the mill center as the charge starts to centrifuge. Therefore the power consumption decreased.

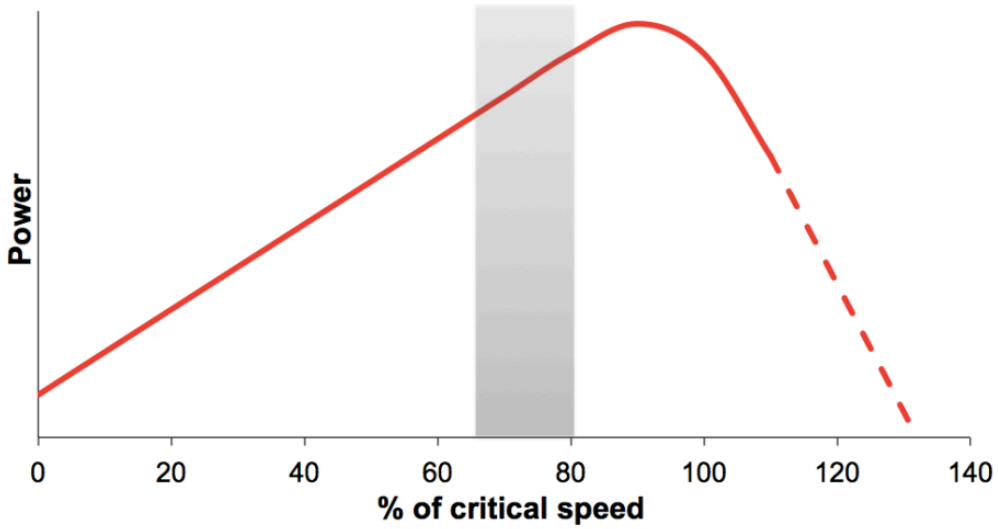

Figure 2.9: Effect of critical speed percentage on power consumption (Francioli, 2015)

The effective operational speed can vary depending on the mill diameter and type of granular materials. It is necessary to conduct a study on effective operational speed of small scale ball mills since the conducted research was at a large scale ball mill.

2.9.3 Mill Filling Charge

In grinding, it is important to know the rate at which the mill drum volume is occupied by grinding media and granular materials. Mill filling is defined as the rate at which the grinding media and the interstices between them occupy the mill volume (Kiangi & Moys, 2008). This parameter can be defined by this relation

$$J = \frac{V_{gm}}{V_m \times (1 - f_p)}, \tag{2.15}$$

where, J, is the mill filling level, V_{gm}, is the volume of the grinding media inside the mill, V_m, is the volume of the mill, f_p, is the fraction volume of interstices between the grinding media usually f_p has a value of 0.4(Francioli, 2015).

The charge inside a mill can be given by:

$$f_c = \frac{V_{ma}}{V_m(1-f_p)}, \tag{2.16}$$

where V_{ma} is the volume of the material inside the mill (Francioli, 2015). The power consumption of a ball mill can also be calculated using Equation 2.17 below

$$P = \frac{2\pi TN}{60}, \tag{2.17}$$

where N is the rotational speed and T is the torque.

The torque necessary to maintain the offset in the center of gravity of the cascading charge from the rest position is given by:

$$T = M_b r_g sin\alpha, \tag{2.18}$$

where M_b is the ball mass and r_g is the distance between the mill centre and α is the angle of repose of the ball charge shown in Figure 2.10.

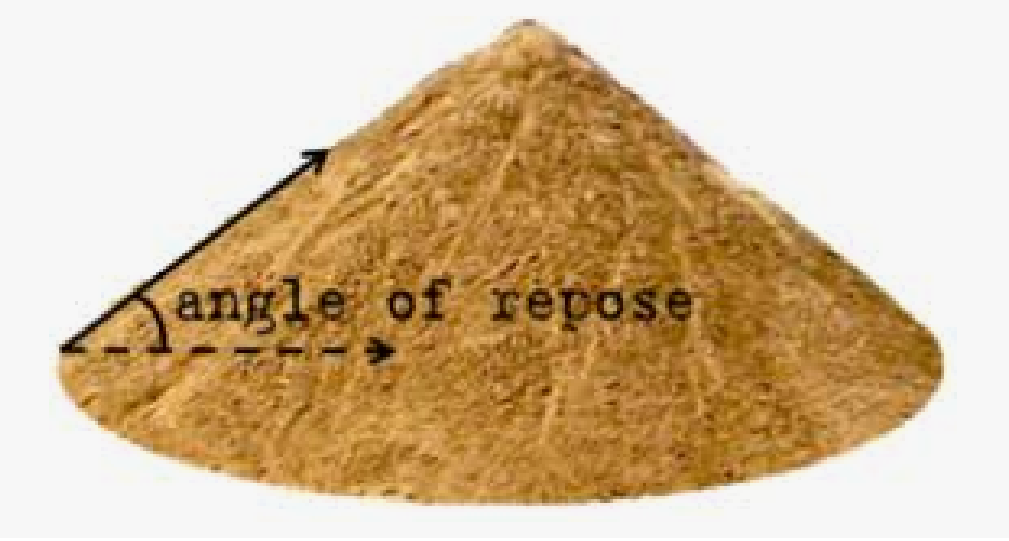

Figure 2.10: Angle of repose

The maximum power calculated is at about 50% ball load. According to Equation 2.18, mill power is a function of ball mass (M_b) and the radius to the center of gravity of ball mass (r_g). As the mill filling increases, the ball mass M_b increases but r_g decreases(Datta et al., 1999). Changing the mill filling can also affect the power consumption. Figure 2.11,

shows that more power is required when charges inside the mill increases in percentage (Francioli, 2015).

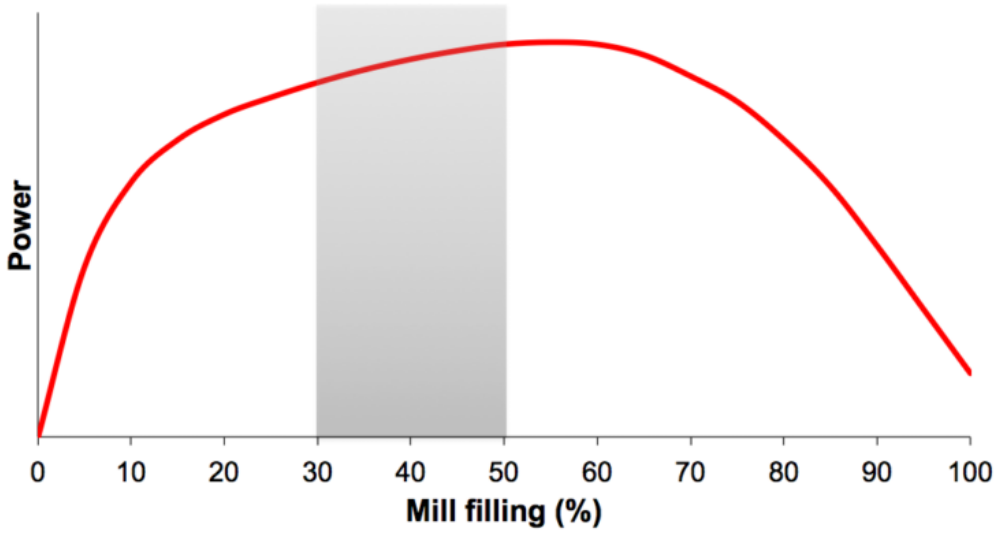

Figure 2.11: Effect of mill filling on power consumption of ball mill (Francioli, 2015)

2.9.4 Media Size

Grinding media size and shape has a significant effect on the grinding operation cost due to huge consumption of liner; thus affect the overall performance of ball mill. The ball size in a mill has a significant influence on the mill efficiency, power consumption and ground material size(Austin & Shoji, 1976; Fuerstenau & Lutch, 1999; Kanda, Simodaira, Kotake, & Abe, 1999). Grinding balls have to provide the maximum stress in the particle, which is greater than the particle hardness. (Ipek, 2007; Kanda et al., 1999) have worked on this problem trying to evaluate the effect of media size on the breakage rate of material and on the power consumption of ball mill.

(Kabezya & Motjotji, 2015)investigated the effect of the ball diameter sizes on milling operation. A laboratory size ball mill was used with different ball media sizes of 10 mm, 20 mm, and 30 mm respectively. The material used to perform the experiment for the experiment. A mill run having a mixture of the 3 ball diameter sizes was also conducted. It was found that, the 30 mm diameter balls were most effective of the three sizes during the grinding of the 3 mono-size feed material samples. The 10 mm diameter balls were the least effective as minimum particle breakage was observed whereas the 20 mm diam-

eter balls were relatively effective to some extent. They also suggested that the mixture of different size of grinding ball can be used for more efficient ball mill. In their findings, mixing the 3 different size of grinding ball, the power consumption for the ball combination mill run decreased and therefore provided the most efficient way of the utilization of power towards particle breakage.

(Magdalinovic, Trumic, & Andric, 2012) also suggests that larger diameter balls consume more energy whereas balls having smaller diameters consume less energy. These different energies are however relative to the optimum ball diameter, which differs according to the size of the mill as well as the desired size reduction of the feed material.

2.9.5 Grinding Media Motion

In mineral grinding, the media motion serves to hit the rock material and break it into small and fine materials. According to (Sun, Dong, Mao, & Fan, 2008), the motion state of practical charge (materials and grinding media) is too complicated to be described precisely. Some researchers considered the grinding media to behave as a single grinding media, while others considered the grinding media as the center of the entire mass which was considered as a rigid body. However, these considerations overlooked some other factors such as the size and shape of particles, this would cause variation between theoretical simulations and experiments.

(Sun et al., 2008), used discrete element method to simulate the motion of grinding media inside the drum of ball mill, which demonstrated that the grinding media motion generates the grinding effect in a cascading motion. The force analysis is crucial for the contact model to analyze media motion by considering grinding media as an individual smooth round spheres (Sun et al., 2008).

2.9.6 Lifters and Liner

Lifters are always fitted onto mill drum not only to protect mill shells but also to enhance the grinding efficiency. They produce a distinct fraction between cataracting load for high energy impact breakage and a velocity gradient within cascading region for abrasion/attrition breakage. However, there is no allowance for lifter designs in all mill power equations (Austin & Shoji, 1976).

The type of liner is driven by the material of construction and applications. For smaller mills, liner has to be handled and installed manually, so smaller blocks with removable

lifters bars are preferred. A list of primary types of liners with their applications, advantages and disadvantages is well described in (Powell & Cleary, 2014) as listed below:

1. Solid Liners
2. Removable lifter
3. Grid Liners
4. Wedged liners
5. Integral wave blocks
6. Uni-Direction profiled liners
7. High–low double wave ball mill liners

Among the seven types of liners, removable lifter is recommended to be used on small scale ball mill, the lifter can be changed rather than the whole liner, thereby maximizing liner life and assisting in manually relined mills. It also allows to change different lifter profile and protect the mill shell.

Other studies conducted by (Makokha & Moys, 2006; Makokha et al., 2007; Makokha, Moys, & Bwalya, 2011) have shown that the liner configuration and lifters has much impact on the breakage rate of the ground materials. The studies were about retrofitting worn liners with cone-lifters. Experiments were performed in a batch wise mode. In all conducted tests, the quartz material was ground for a total period of 4 min.

Assessment of the performance of the three liner profiles under investigation and a comparison of the grinding data was made to which a conclusion was made that the liner profile significantly influences the milling rate and fines production in the mill.

Figure 2.12, also shows another study conducted by (Yin et al., 2017), showing the effect of lifter height. It can be observed that lifter height has less significant effect on power consumption of ball mill.

(Moys, Van nierop, Van Tonder, & Glover, 1998), conducted the study to predict the forces exerted on the lifter bar using DEM. (Van Nierop et al., 2001), also analyzed the power draw and overall charge motion. In all these work, only square lifters were used.

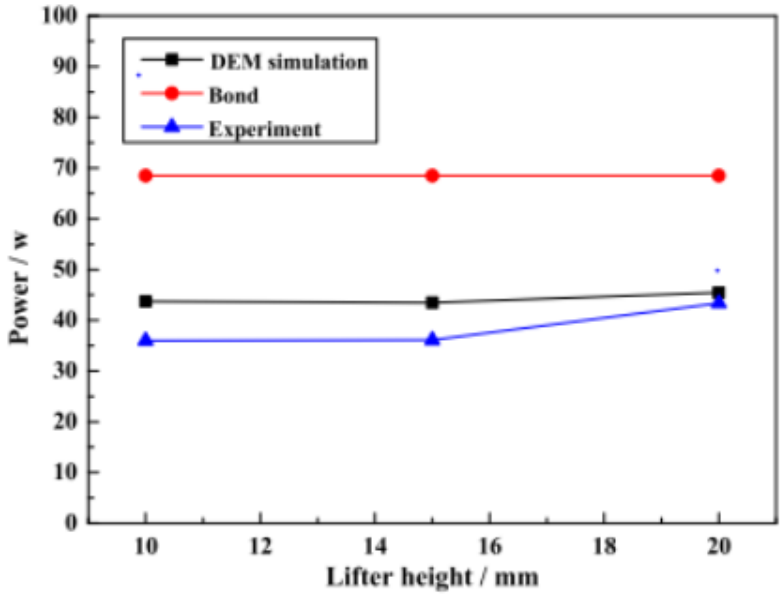

Figure 2.12: Power draw at different lifter heights(Yin et al., 2017).

(Hlungwani et al., 2003), investigated two types of lifter profile square and trapezoidal lifters in terms of power draw and load behavior with a 2D model. It was observed that trapezoidal lifter drew more power than square lifters. However the shape of lifter profile keeps on changing as the lifter contact face is wearing. It is therefore needed to incorporate a 3D model and investigate other lifter profiles.

(Cleary & Morrison, 2011b), investigated the energy consumption of a laboratory scale ball mill using DEM. The aim was to understand the ore breakage by exploring the effect of media charge powder fill level on the power draw. A cylindrical drum of 435 mm inner diameter was with six square lifters. A constant mill speed of 41 rpm which is 64% of critical speed was used. It was found that small lifters in height collect and lift the concentration of the ore particles and increase the fall of ore particles at the toe and lower the power draw. However, the effects of lifter configurations (shape, number of lifters) were not investigated.

(Bian, Wang, Wang, Wang, & Lv, 2017), investigated the effect of lifters and mill speed on particle behavior, torque, and power consumption. A 3D model was used for trapezoidal lifter, and concluded that the torque is affected by lifter height, lifter number, and mill speed. However, the research did not investigate other lifter profiles effects and how they affect power consumption.

2.10 Summary of Gaps

This chapter reviewed the evolution of ball mills as well as the parameters that affect the grinding process. It was observed that, to achieve a great impact of the grinding media and minimum power consumption, it is essential to account for mill diameter, mill speed, mill filling volume, media size distribution and lifter configurations that influence the grinding process as listed above. Even though a number of researchers have investigated a number of these parameters, little attention has been focused on lifter configuration and their effect of the grinding process. The following gaps were identified from the reviewed literature.

1. Researchers have investigated the effect of mill diameter on power consumption. In all reviewed studies, the number of lifters that can be fitted in one specific mill diameter has not been adequately addressed.

2. A significant amount of work has been carried using square configuration of lifters. However, the lifter profile keeps on changing as the lifter contact face is wearing. It therefore important to evaluate other lifter profile and their effect on the grinding process.

3. It is documented that grinding media size and their size distribution have a great impact on the fineness of particles. However, effective size distribution for a certain mill filling level has not been investigated as per reviewed literature.

This research is aimed at addressing the first and the second gaps.

CHAPTER THREE
METHODOLOGY

3.1 Introduction

This chapter presents a description of different methods that were employed to analyze the power consumption and the impact load using a small scale ball mill. The main purpose of this research is to optimize process parameters of a small scale ball mill by reduction of power consumption and fineness of ground particles. Hence providing optimal grinding parameters through simulation using discrete element method.

A geometric mode of the small scale ball mill has been developed to mimic operations of the ball mill. The main parts :*mill drum, frame, liner and lifters* were assembled using Autodesk Inventor 2017 software.

Numerical simulations were conducted in discrete element software EDEM. A simplified geometry was imported in EDEM software together with materials to be ground. A number of simulations were conducted to analyze the effect of different parameters after which experimental validation were conducted at JKUAT workshop. Conventional circular surface profile liner was modeled with different lifter profiles. The performance of each lifter profile was analyzed, using single size spherical grinding media (balls) created in EDEM.

3.2 Selection of Parameters

The parameters used in this research were selected refering to the existing ball mill built at JKUAT. It is a cylindrical ball mill of 372 mm diameter and 556 mm of length and it has 4 rectangular lifters. This was selected as the base condition, thereafter, all other paramaters were varied according to the progress of the results. Lifter configuration was changed on the basis of contact face angle. The width of 20 mm and height of 20 mm of lifter profile were kept constant for all lifter profiles and they were used to calculate the respective face angles, 0, 14.04, 26.56 degrees for rectangular, trapezoidal, and triangular lifters respectively. The number of lifter were changed ranging between 2 and 12 with an increment of 1. This was done to eveluate the effect of lifter number on power consumption and to provide the optimum number of lifters for this small scale ball mill. The height of lifters was changed from 0 to 30 mm with an increment of 10. The critical speed of the drum were calculated using equation 3.2 and the variation in percentage of critical speed was

done refering to the range of effective grinding review in the literature.

3.3 Design of Experiment

Full factorial design using two levels factorial with specified generators was used in Minitab 17 software. The number of factors used were 4; lifter profile, lifter number, lifter height, and mill speed. The total number of experiments were 21 as can be seen in Table 3.1

Table 3.1: Desing of experiment

Lifter profile	Lifter height	Lifter number	Critical speed
0	10	12	65
12.5	20	7	75
12.5	20	7	75
12.5	20	7	75
25	10	12	65
0	30	12	85
0	10	2	65
25	10	2	65
0	30	2	65
25	30	2	65
0	30	12	65
0	10	2	85
0	30	2	85
25	30	2	85
0	10	12	85
25	30	12	85
12.5	20	7	75
25	30	12	65
25	10	12	85
25	10	2	85
12.5	20	7	75

3.4 Geometric Modeling.

Geometrical modeling comprises of describing the shape of a certain object by using computer aided design software. A small scale ball mill was designed using Autodesk inventor 2017. The main parts of physical models were completed as can be seen in Figure 1.1.

3.4.1 Drum Geometry

The cylindrical drum of a ball mill comprises of the liner and lifters. The volume of the drum can be estimated from the quantity of materials that is needed to be ground. Refering to the survey report by RPE in JKUAT (Kyalo et al., 2017), Migori county in Kenya have artisanal miners who are facing non mechanisation problem in their mining activities. Based on this survey, a drum geometry for the capacity of 60 liters (0.06 m^3) was selected to be used in mineral processing. Ball mills are restricted to those having a length to diameter ratio of l.5 to 1 whereas for tube mills, the length to diameter ratio is between 3 and 5 (B. Wills, 1993). A ratio of length to diameter of 1.5 was used to determine the total volume of the mill drum. This was done to have the maximum volume of the drum.

$$V = \frac{\pi {D_m}^2 L}{4} \tag{3.1}$$

where V is the volume of the drum, D_m is internal diameter of mill and L is the length of mill. The volume of the drum determines the internal mill diameter, the critical speed of the drum, and the mill charge volume. The critical speed Cr of a rotating mill was computed using Equation 3.2 below (Kobayashi, 2007).

$$Cr = \frac{42.3}{\sqrt{D_m}} rev/min. \tag{3.2}$$

The normal specific rates of breakage vary with respect to the change in mill speed. However, the maximum power consumption usually occurs within the range of 65-85% of critical speed (Usman, 2015). The operational speed range used in this research was 65-100% of the critical speed to analyze the impact of balls motion on power consumption for a small scale ball mill at operational speed.

The grinding media charge volume in mill, V_{gm} is defined as a fraction of the total interior mill volume occupied by grinding balls, which was calculated using Equation 3.3 (Ene, 2007), where D_m is the inside diameter and H is the vertical distance down from the inside top of the mill to the leveled grinding charge (see Figure 3.1).

$$V_{gm} = 112.5 - 125\frac{H}{D_m}, \tag{3.3}$$

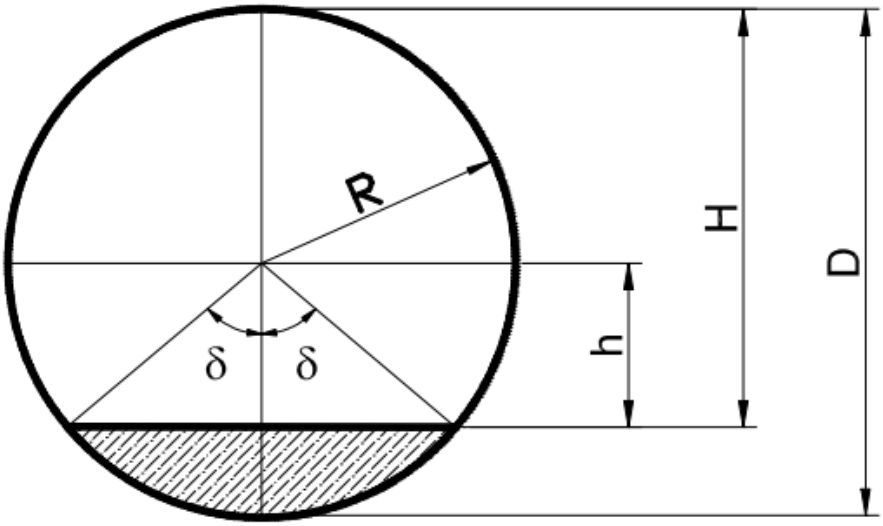

Figure 3.1: Height levels of ball mill filling (Ene, 2007)

The height of the free space in mill H is equal to:

$$H = (h/D_m + 0.5) \times D_m, \tag{3.4}$$

The volume occupied by the grinding media together with the interstices between them J was calculated using Equation 3.7 whereas the volume of emptiness also known as powder filling volume was calculated taking the volume occupied by the grinding media together with the interstices minus the volume of grinding media shown in Equation 3.5

$$U = J - V_g m = \frac{f_c}{f_p \times J}, \tag{3.5}$$

The effective mill volume is equal to the volume of the drum minus the volume of the liner and volume of lifters as shown in Equation 3.6

$$V = V_i - (V_L + V_l). \tag{3.6}$$

Where, V is the effective volume of the drum, V_i is the internal volume of the drum, V_L is the volume of the liner, and V_l is the volume of the lifters. The summary of the volumes are presented in the Table 3.2

Table 3.2: Effective volume of drum

No	Parts	Volume(m^3)
1	Drum Internal	58.69 x 10^{-3}
2	Drum cylinder liner	3.11 x 10^{-3}
3	Side liners	1.82 x 10^{-3}
4	Lifters	1.04 x 10^{-3}
5	Effective Volume	52.71 x 10^{-3}

In this research, the power consumption was analyzed using a mill filled with balls mixed with ore particles, experimentally and numerically. A summary of grinding condition can be seen in Table 3.3.

Table 3.3: Ball drum grinding conditions

Specification	Quantity	Dimensions
Mill	Diameter,D(m)	0.372
	Length, L(m)	0.5565
	volume, $V_m(m^3)$	0.06
Mill speed	Critical speed(rev/min)	69.35
	Operational speed (rev/min)	54
Grinding	Diameter, d(mm)	10
	Specific gravity (g/cm^3)	7.85
	Ball-filling volume $(\%)$	40
	Fraction $J(\%)$	41

A full scale ball mill was used to conduct experimental work. (Djordjevic et al., 2004), demonstrated that a cylindrical ball mill can be represented by a slice. A sliced cross section of the full scale has been used in simulations to reduce the number of balls which lead to an intense computational power.

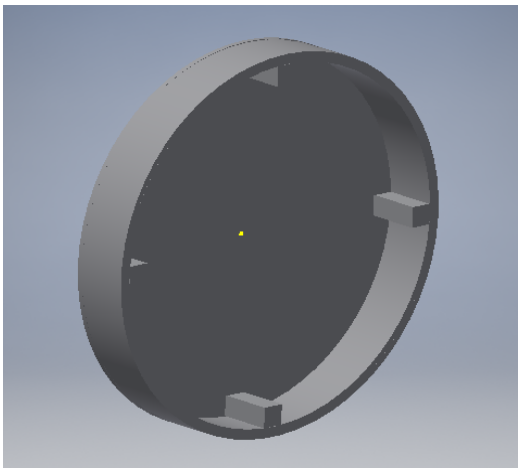

(a) CAD model in Autodesk Inventor 2017

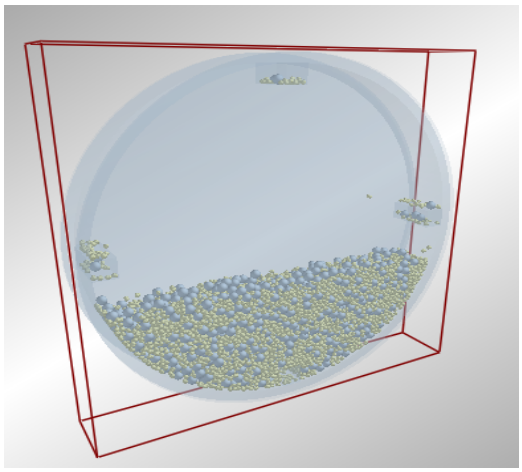

(b) Screen capture shot of drum model in EDEM with 40% charges

Figure 3.2: A sliced cross section of the full scale drum

The actual ball mill used has an internal diameter of 0.372 m and length of 0.556 m. A sliced cross section was used to reduce the computing time, instead of the full scale mill, only a 0.05 m axial slice was used as shown in Figure 3.2. The results obtained were multiplied by the ratio of total mill length to the slice length. This gave the total values of related parameter for the full scale mill.

3.4.2 Liner and Lifter Modeling

Poor lining of a ball mill design has a detrimental effect on the overall mill performance and on liner life (Powell & Cleary, 2014). It results not only in loss of revenue and increased operational costs but also reduce milling efficiency. This can result in excess power usage and decreased recovery of the valuable minerals. Since the liners and lifters are among the parameters that significantly affect the power consumption in the mill (Fuerstenau & Lutch, 1999), there is a need to study the effect of lifters geometry in a small scale ball mill.

1. Lifter Profile

   In this study, five lifter profile were investigated to analyze their effect on the power consumption and impact load by a small scale ball mill. Rectangular, trapezoidal, triangular, parabolic and round lifters have been drawn as shown in Figure 3.4, and 3.3.

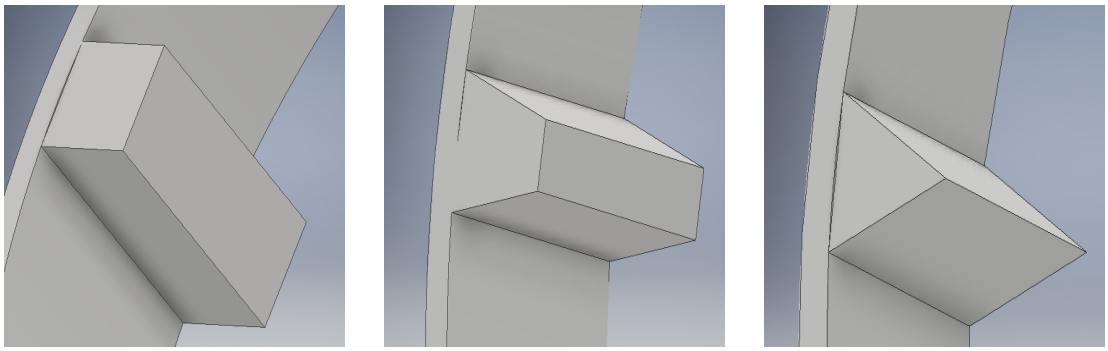

(a) Rectangular (b) Trapezoidal (c) Triangular

Figure 3.3: Polygonal lifters with 20 mm width and 20 mm height

(a) Parabolic (b) Round

Figure 3.4: Curved face lifters with 20 mm width and 20 mm height

The lifter profiles are distinguished by their contact face to the vertical plane. The face angle was calculated by using the height and width of the lifters shown in Appendix III. The contact faces are normally flat surface or curved surface that lift the grinding balls higher to increase the height of falling. In this study two types of contact faces have been used; Polygonal lifters that have flat contact face and curved contact face lifter in Figure 3.4.

2. Number of Lifters

   The number of lifters is another parameter that affect the power consumption of ball mill. The motion of grinding media (balls) depends on the volume of the grinding mill which may be affected by the number of lifters. When number of lifters increases the inner volume of the drum decreases and the inter-space between two connective lifters also decrease. Table 3.4, illustrates the lifter configuration used in

this research. The number of lifter was set from 2 to 12, with an increment of 1 as can be seen in Figure 3.5

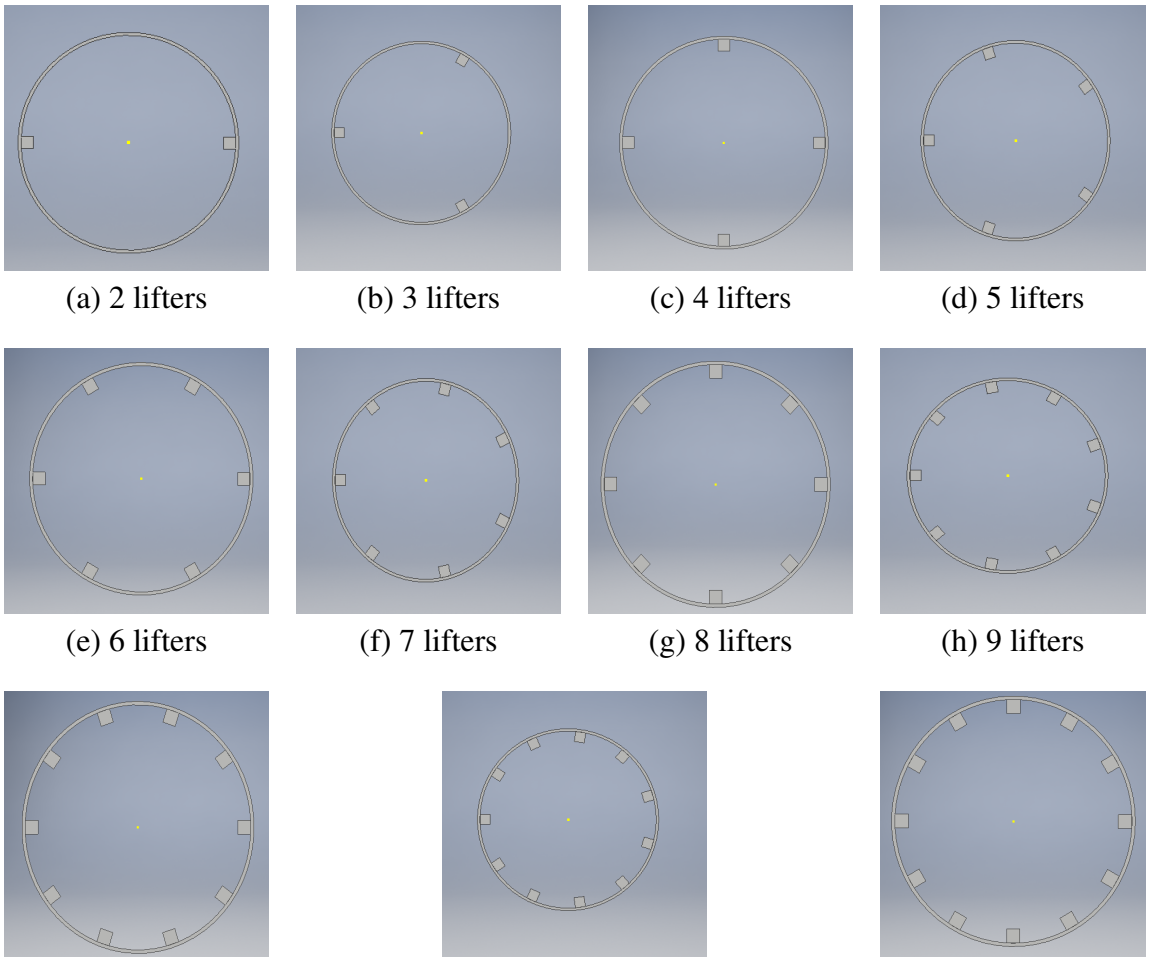

(a) 2 lifters (b) 3 lifters (c) 4 lifters (d) 5 lifters

(e) 6 lifters (f) 7 lifters (g) 8 lifters (h) 9 lifters

(i) 10 lifters (j) 11 lifters (k) 12 lifters

Figure 3.5: Number of lifters used in simulation

3. Height of Lifters

   In grinding process, lifters play a great role of lifting up the grinding balls, and when the balls fall back they hit the mill wall as well as the lifter. This process leads to the wear of lifters and decrease their height. It has been shown that the height of lifter affect the lifting of balls inside the drum (Djordjevic et al., 2004). In this study, the lifter height was set to $0, 10, 20$, and 30 mm as it can be seen in Figure3.6. This was done due to the observation in the review literature that showed that incresing lifter heigth has slight increase in power consumption. Table 3.4, summarizes the

lifter configuration and speed used on each profile. The lifter height of parabolic and round lifters was not caluculated. This was due to their effect in power consumption and impact load by considering their profile and the number of lifter. Hence they were not used in the analysis of power consumption considering lifter height and mill speed.

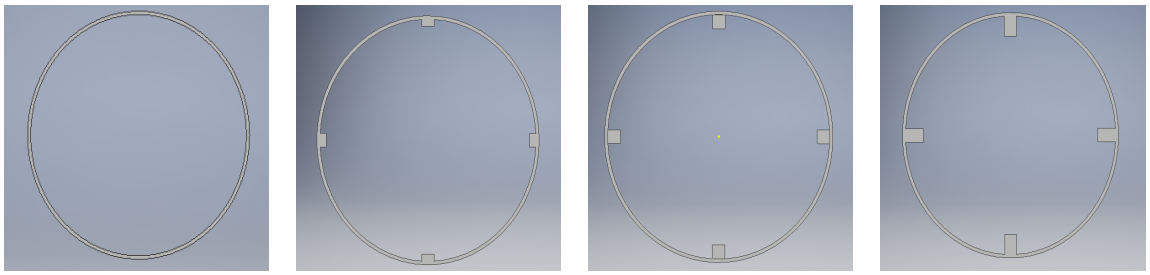

(a) Height=0 mm (b) Height=10 mm (c) Height=20 mm (d) Height=30 mm

Figure 3.6: Height of lifter used in simulations

Table 3.4: Lifter configuration used in DEM simulation

Cases	Lifter profiles	Lifter number	Speed in %	Height	Face angle
1	Rectangular lifters	2-12	65-100	0, 10, 20, 30	0
2	Trapezoidal lifters	2-12	65-100	0, 10, 20, 30	14.04
3	Triangular lifters	2-12	65-100	0, 10, 20, 30	26.56
4	Parabolic lifters	2-12	65-100	20	-
5	Round lifters	2-12	65-100	20	-

3.4.3 Grinding Media Models

Grinding media is composed of numerous balls sometimes of different size. (Fuerstenau & Lutch, 1999), have shown that the ball size in ball mill plays a significant influence on the mill throughput as well as on the power consumption. This ensures that grinding media size distribution has a great impact on the overall performance of the ball mill.

Choosing the materials to be used in making the ball, steel as compared to the best option. Steel is a mixture of several metal or alloy and most of it is iron. The grinding balls used in this study were of single size of 10 mm diameter for simulation and 25.4 mm for experimental analysis. The balls used in experiment were steel balls sourced from local cement company, their composition was tested using X-ray fluorescence (XRF) machine and it was 79.6% of Iron 14.54% Chromium, 3.68% of Carbon, then Manganese.

The necessary number of balls having the definite diameter Nb in a mill should be proportional to the volume of charge(J), as shown in Equation 3.7. The number of balls used in simulation was 1197 computed by assuming 40% of the volume of the drum.

$$Nb \approx J \tag{3.7}$$

3.5 DEM Simulation of Small Scale Ball Mill

In this study, DEM was used to numerically analyze interaction of particles in small scale ball mill. EDEM software 2.7 version (EDEM® from Dem Solutions Ltd.) was used to carry out the DEM simulations. The results obtained from the DEM simulation were analyzed using Orgin Pro 9.1 software.

3.5.1 Simulation Parameters

In this study, the mill geometry was modeled based on the mill built at JKUAT, Kenya (illustrated in Figure 3.7). The drum geometry was sliced to 50 mm long to reduce the computational power. The paramaters that were modelled was shown in Table3.5

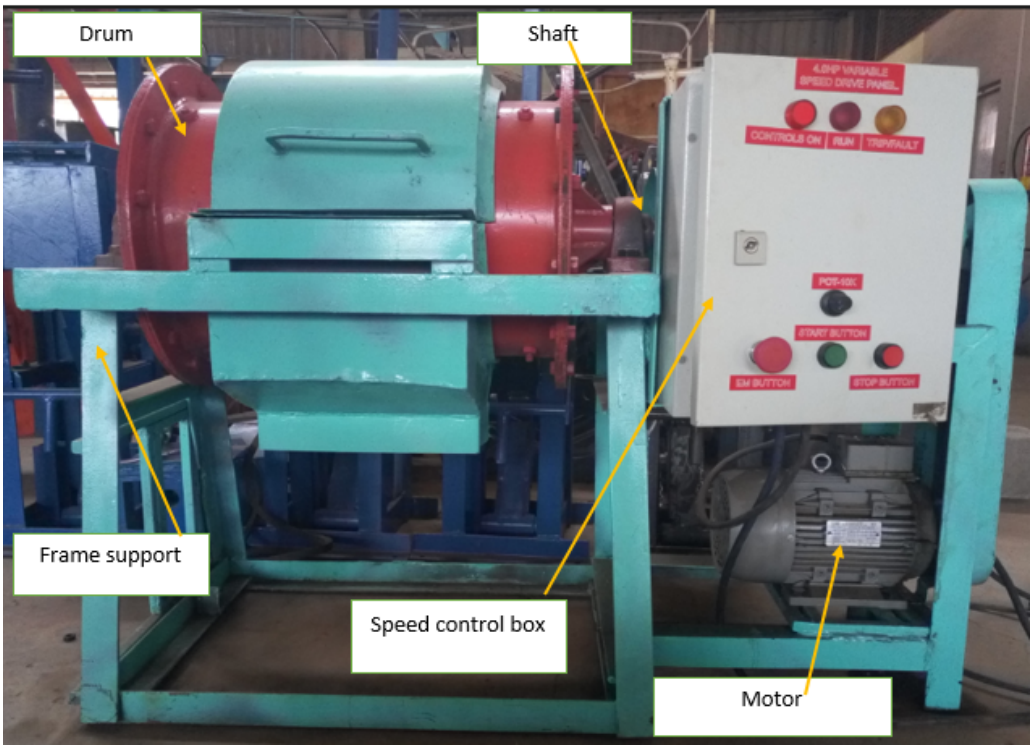

Figure 3.7: Ball mill built in JKUAT

A drum geometry of the mill had 4 rectangular lifters, 40% mill filling, rotating at 75% of the critical speed was selected as the base condition, thereafter, all other simulations were changed according to the progress of the results and the need to conduct many other tests using different parameters evaluate many tests with different operational variables.

Table 3.5: Geometrical parameters for full scale and sliced drum

Parameters	**Full drum**	**sliced drum**
Diameter	0.372 m	0.372 m
Length	556 mm	50 mm
Lifter profile	Rectangular	Rectangular
Lifter Width	20	20
Lifter Height	20	20
Number of lifters	4	4

EDEM allows the user to import a CAD geometry saved in (*.iges) format. The sliced geometries of different lifter profiles were constructed using Autodesk Inventor 2017 and saved in CAD exchange format to be imported in EDEM.

Table 3.6: Material properties and interaction parameters (Kulya, 2008)

Material properties			**Interaction parameters**			
	Balls	Ore		Balls-balls	Ore-Ore	Balls-Ore
Poisson's ration	0.3	0.5	Coefficient of restitution	0.5	0.3	0.5
Shear modulus(pa)	7.50E+08	4.50E+07	Coefficient of static friction	0.74	0.8	0.5
Density (kg/m^3)	7800	2500	Coefficient of rolling friction	0.002	0.005	0.003

The material properties presented in this study Table 3.6, were adopted from (Kulya, 2008) who experimentally calculated material properties for steel balls interactions. In this study, grinding media together with quartz particles were used. The number of ore particles together with grinding media was 8000 which is 40% of the volume of the drum . The operational speed was set to be (65-100 %) of the critical speed as it can be seen in Table 3.4.

3.5.2 Simulation Set Up

Simulation was conducted in the following steps:

- Step 1: The simulation parameters were defined from the material properties such as Poisson's ratio, density, shear modulus, and material interaction parameters as shown in Figure 3.8

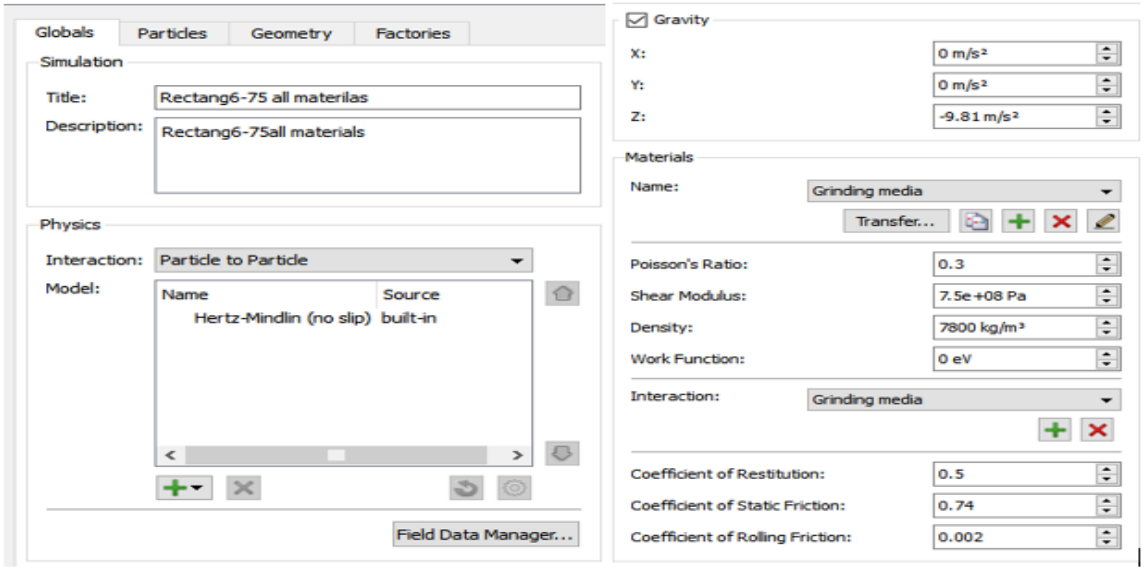

Figure 3.8: Global setting for material properties and interaction in EDEM

- Step 2: The particles were defined in EDEM as spherical particles whereas the particles were created as it can be seen in Figure 3.9, the diameter of the steel ball and the particles were 10 mm, and 4 mm respectively.

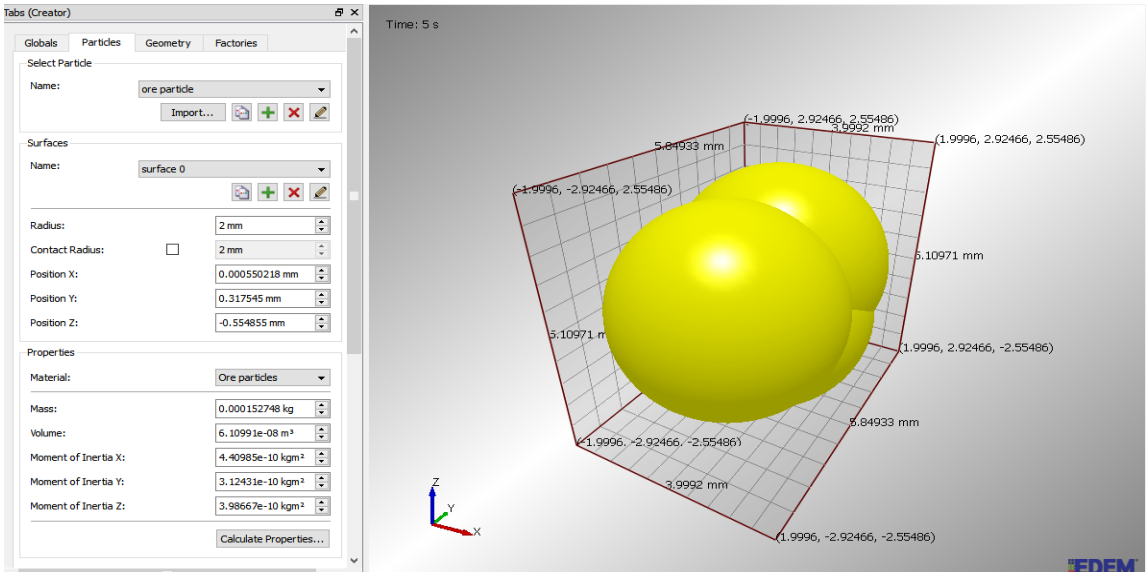

Figure 3.9: Particles created in EDEM

- Step 3: The geometry was imported into EDEM, with the material of the geometry was set and speed was in rad/s. The periodic boundaries of particle factory were set in x, y, and z directions. The particles are constrained in this factory and will be

rotating within the created boundaries.

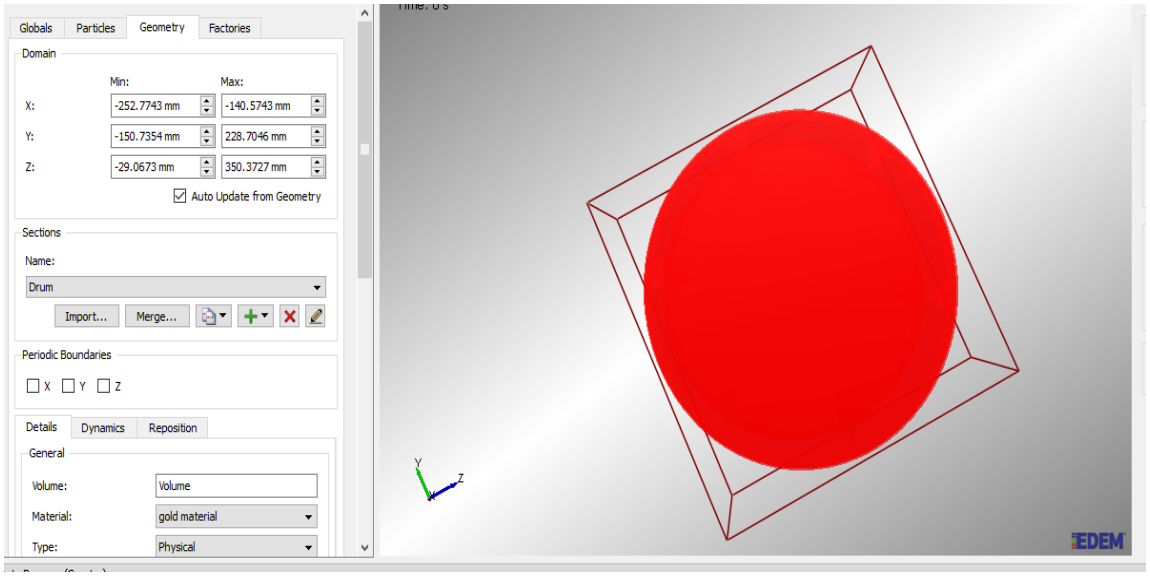

Figure 3.10: A sliced drum imported in EDEM

- Step 4: The particle factory was defined, the number of particles were included at this stage. A static factory means that particle are created at the start of the simulation and the dynamics of particle will be created during the simulation (illustrated in Figure 3.11).

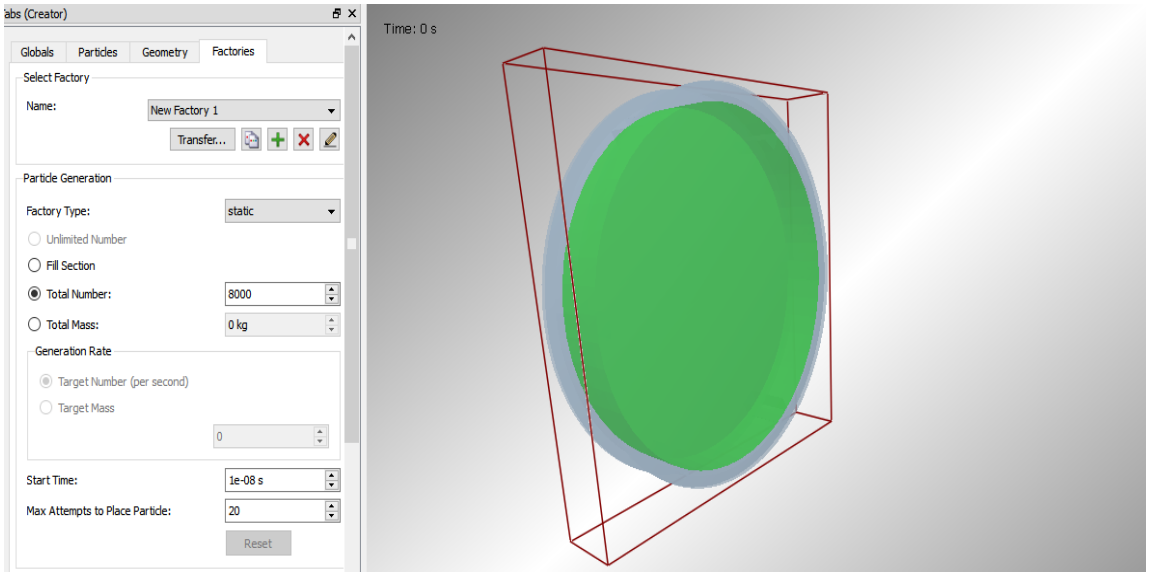

Figure 3.11: Static particle factory setting used in EDEM

- Step 5: The simulation were run. The simulation time was set to be 5 sec, time step was set to be 20% of Rayleigh time step 2.3261×10^{-6} illustrated in Figure 3.12

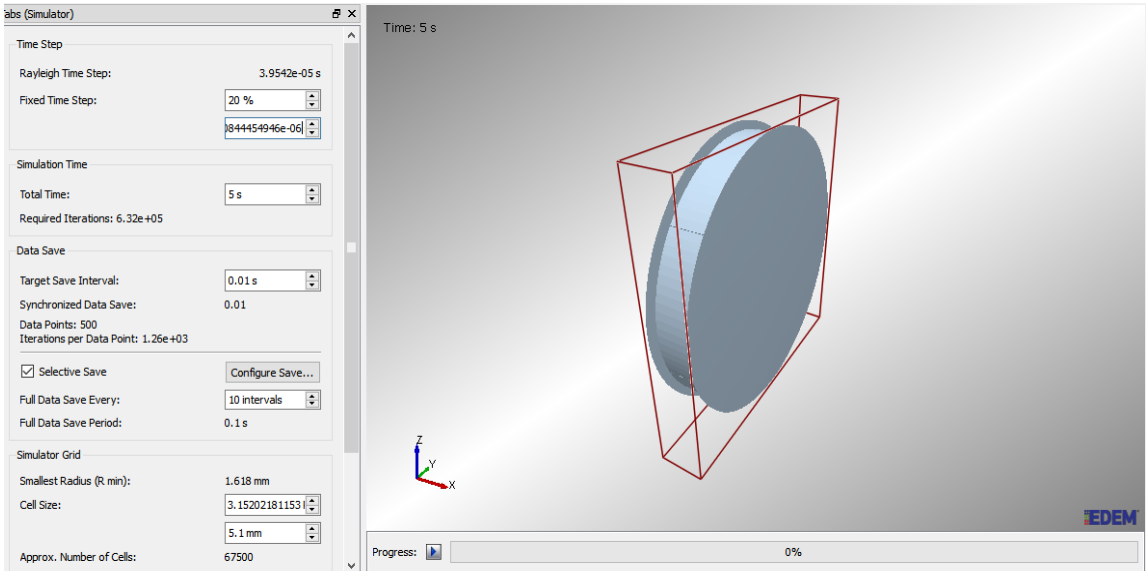

Figure 3.12: Screen capture of simulation set up used in EDEM software

- Step 6: Analysis of the simulated parameters was conducted using EDEM software. Torque and impact force data was exported in (*.csv format) to Microsoft Excel. Figure 3.13 illustrate the particle motion in EDEM.

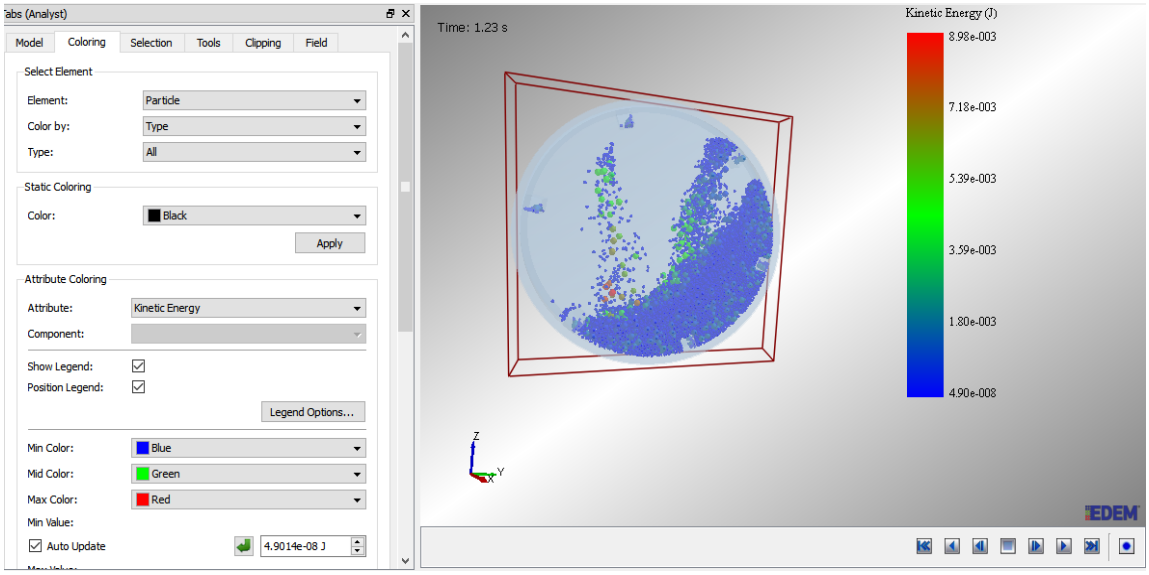

Figure 3.13: Screen capture of particle motion in EDEM software

The power consumption and impact load were imported from the software and analyzed in Microsoft Excel.

3.6 Stability of the Simulation Model

The numerical stability of EDEM model depends on the time step selected. The time step is defined as the amount of time between iterations. It is fixed and remains constant throughout the simulation. It is displayed as actual time in seconds as percentage of Rayleigh time step. The Rayleigh time step is the time taken for shear wave to propagate through a solid particle.

Table 3.8: Variation of power with the change in time step

% of Rayleigh time step	Power (Watts)	% of Rayleigh time step	Power (Watts)
5	187.87	30	223.69
10	189.88	35	238.097
15	189.58	40	266.60
20	190.23	45	17717.89
25	211.76	50	112942.77

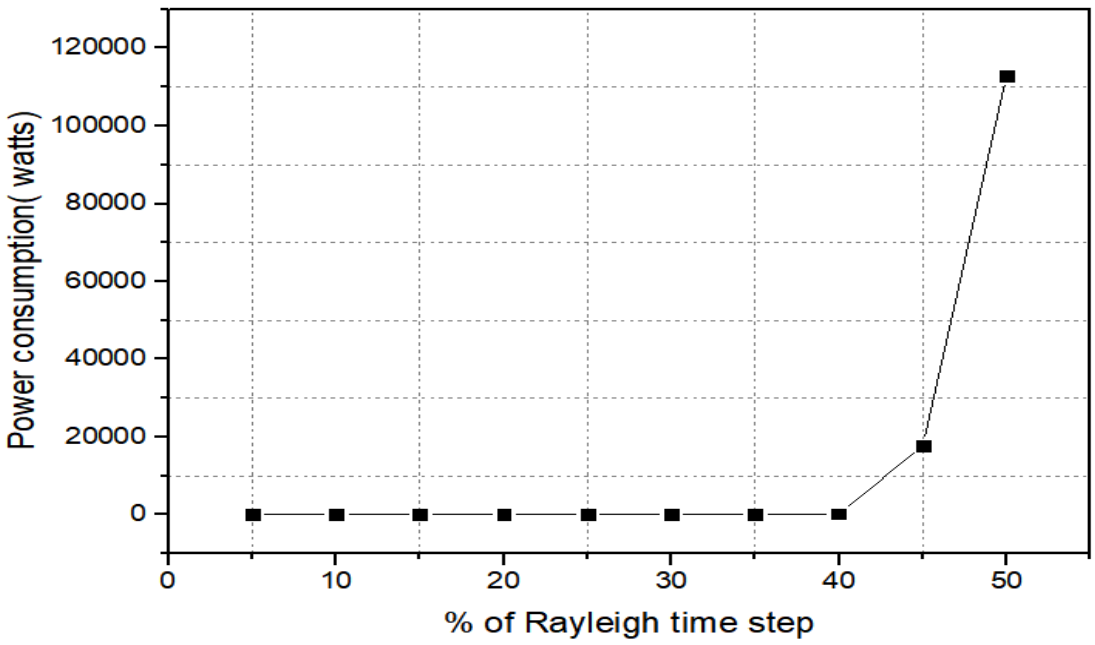

Figure 3.14: Stability of EDEM model

It recorded that the smaller the time step, the longer the simulation time (DEM Solutions, 2011). Figure 3.14 and Table 3.8, illustrate the effect of time step change to the power consumption, when the time step is too large, it will lead to numerical instability and may cause exploding of particles as the overlap and forces on particles get too large. The main

reason is that when the particles interact, the collision needs to be resolved over a number of time steps. If the time step is too large, the force calculation is not accurate enough to give true representation of interaction process. The time step used in this study was set at 20% of Rayleigh time step. The reason is that, the model is stable at this time step and the simulation time is not too high.

The main computational challenge in DEM simulation is the detection of contacts. By dividing the domain into grid cells, the simulator can check each cell and analyze only those that contain two or more elements (and therefore a possible contact), thus reducing processing time. As the grid length decreases, fewer elements are assigned to each grid cell and contacts become easier to resolve. The fewer particles per grid cell, the more efficient the simulator. The grid cell used in the simulation was 3 Rmin where where Rmin is the minimum particle radius in the simulation.

3.7 Experimental Set Up

In this study, a small scale ball mill built at JKUAT was used. It was used to validate the power consumption obtained from simulations with experiments for a ball mill with rectangular lifter. A set of experiments were conducted as illustrated in Table 3.9.

Table 3.9: Experimental details

Charge(%)	speed(%)	Time(min)
40	65	5
	70	5
	75	5
	80	5
	85	5

The aggregates of Basalt of size ranging between (4-7 mm) were used for a set of four batch grinding. The mill filling volume was set to be 40% same as in simulations. The total grinding time was set at 5 min, speed set to be 65-85% of the critical speed. Mono-size balls of (25.4 mm) in diameter were used to grind the Basalt materials. Table 3.10, illustrates volumes used in experiments.

Table 3.10: Experimental detail of batch grinding

No	Parameters	volume (mm^3)
1	Effective volume of the drum	52.71 x 10^6
2	Volume of grinding media	21.08 x 10^6
3	Volume of a single ball	8.58 x 10^3
4	Volume of basalt	3.77 x 10^6

In each experiment, the mill products were discharged and then subjected to sieving and analysis using vibrator sieving machine. The power consumed by the ball mill at the given operating time was measured by a Fluke 1735 power logger which automatically captures and logs over 500 power quality parameters. It has best voltage measurement accuracy of $\pm$ 0.15 %, best current measurement accuracy of $\pm$ 0.5 % and power factor accuracy of $\pm$ 1% of full scale (Corporation, n.d.).

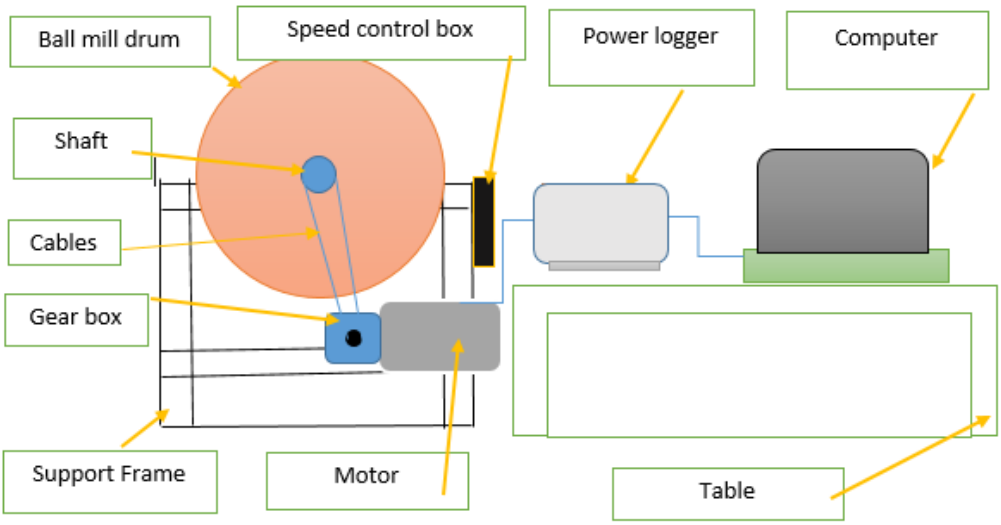

Figure 3.15: Expermental set up for a small scale ball mill

Figure 3.15 illustrates the experimental set up that was used in this study. A power logger connected to the motor to measure the power consumption when the ball mill was grinding. The active power that was recorded through the power logger was exported in the computer for analysis.

3.8 Validation of Simulation Results

A geometrical model was modeled as per the actual ball mill model bulit at JKUAT. The mill filling rate, mill speed, grinding media size, lifter profile, number of lifters, and lifter

heigth were set to be identical in both simulation and experiments as shown in Table 3.11. The grinding time was set to 5 min after which the power consumption from both simulation and experiments were analyzed.

Table 3.11: Validation detail of both simulation and experiment

Parameters	Simulations	Experiments
Lifter profile	Rectangular	Rectangular
Lifter Number	4	4
Lifter Height	20 mm	20 mm
Grinding media size	25.4 mm	25.4 mm
% of critical speed	65-85	65-85
Mill filling rate	40%	40%

3.8.1 Comparison of Simulated Results and Experimental Results

Many assumptions have been made in simulating the interaction of grinding balls inside the drum and the effect of different lifter profiles and mill speed. It is therefore important to validate the DEM model using experimental analysis. In this section, results of the simulation and experimental data were compared.

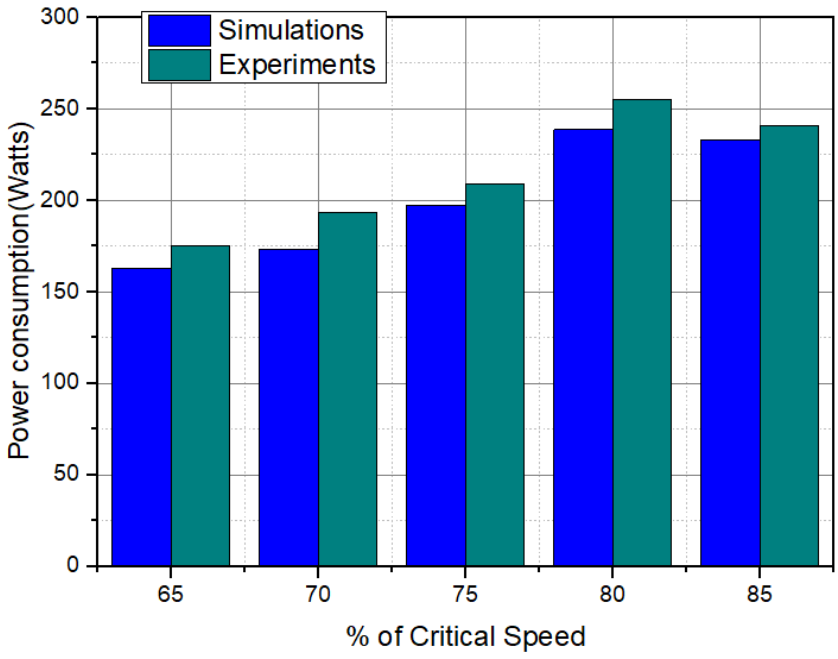

Figure 3.16: Comparison of experimental results with simulation results

Figure 3.16 illustrates the simulation data and experimental data using 40 % of mill filling and 4 number of lifters. It was observed that, the power consumption increases as the speed increases. The maximum power consumption was found to be at 80% of the critical speed. DEM was able to predict the power consumption and the interaction of particles in a small scale ball mill. The discrepancy between the experimental results and simulation results can be attributed to the assumptions made during DEM simulations.

Table 3.12: Comparison of simulation results with experimental

Speed (%)	**Simulations (Watts)**	**Experiments (Watts)**	**Error** (%)
65	162.57	175	7.03
70	173.8	193	10.21
75	197.06	209	5.71
80	238.12	255	6.46
85	233.01	241	3.31

The average error of 6.54 % obtained from the Tables 3.12 can be attributed to the following assumptions made in DEM simulations:

- All particles inside are of the same size and shape.
- There is an equal distribution of collision energy between particles and grinding balls.
- All particles have the same mass
- There were no fine particles in the simulation
- Perfect mixture of particles
- All particles are broken in similar way
- The material properties used in simulations are the same as the material properties used in experiments.
- The power losses from transmission system is not included in the EDEM simulations.

All those assumption can results into errors. The same trend were observed in the work of (Bian et al., 2017) who experimentally validated the simulation results and obtained the error difference of 10.1%.

CHAPTER FOUR
RESULTS AND DISCUSSION

4.1 Introduction

This chapter presents analysis and discussion of results that were obtained from both DEM simulation and experiments. The validation of simulation results was conducted by comparing the power consumed by a mill having 4 rectangular lifters both in simulation and experiment. The effect of lifter geometry was investigated using five lifter profiles; three of them having flat contact surface and two having curved surface. The number of lifters used in simulation were ranged from $0-12$, with an increment of 1. The lifter height varied from $0-30$ mm range and the mill speed from 65-100% of the critical speed. Experimental results were obtained considering rectangular lifter profile as discussed in Section 3.7

4.2 Effect of Lifter Profile

4.2.1 Effect of Lifter Profile on the Power Consumption

Lifters are fitted into the mill drum to protect mill shells and enhance the lifting of grinding media hence improve the grinding efficiency. However, mill power equations proposed in the literature do not consider the lifter geometry. In this study, five lifter profiles shown in Figure 3.3, and 3.4 were evaluated numerically using discrete element method (DEM). All the simulations in this study were conducted in a 372 mm diameter drum.

Parameters used in this study were adopted from the literature for the best performance of ball mill operating at mill filling level $J = 40\%$ and operational speed $\phi = 75\%$ of the critical speed (V. K. Gupta & Sharma, 2014; Petrakis, Stamboliadis, & Komnitsas, 2017). Figure 4.1 shows the numerical results for 4 lifters for different lifter profiles.

The power consumption was found to depend on the face angle, with reference to the vertical plan, increasing slightly as the face angle increases. The average deviation of power consumption was found to be 8.53 watts. The power consumption of lifters with flat surface was found to be less compared to lifters with curved contact surface. Lifters raise up the balls and lift them higher to increase the height of fall and the kinetic energy of the balls. The reason is that rectangular lifters have zero face angle, which when balls are lifted up, balls and particles will easily be propelled to the contact point, toe and this prevents

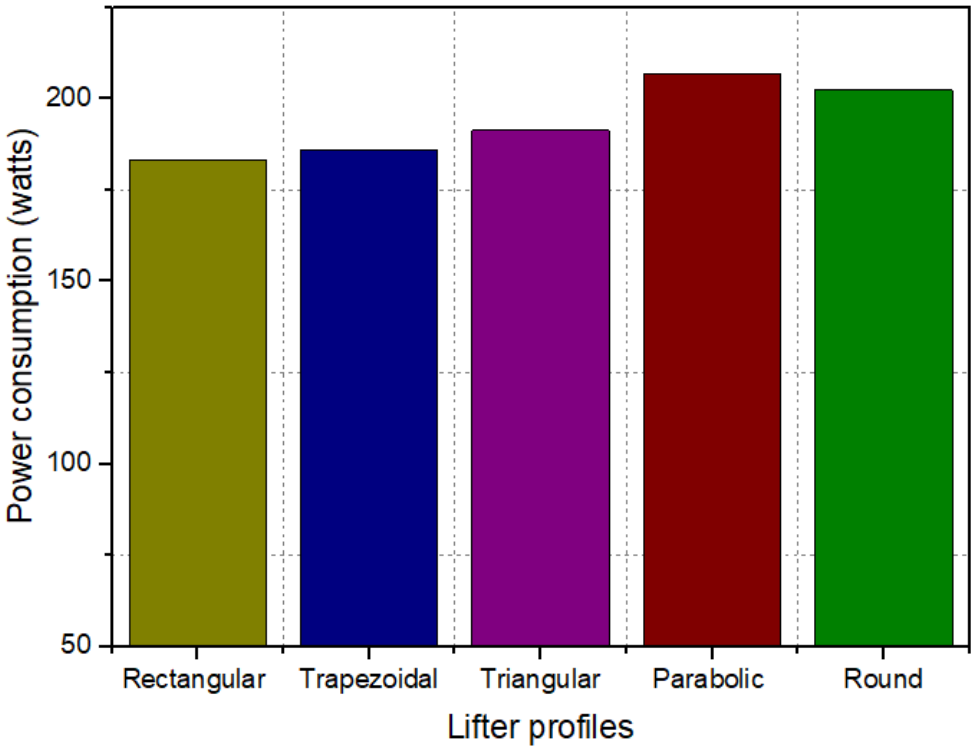

Figure 4.1: Power consumption for ball mill with different lifter profile

excessive use of torque to lift up the materials, thus result in less power. When the face angle is increased to make a trapezoidal lifter (face angle= 14.04^0), the torque required to lift materials also increases which also increase the power consumption. This observation agrees with the findings of (Hlungwani et al., 2003) who observed that trapezoidal lifters draw more power than the square lifters.

Triangular lifters consumed more power compared to rectangular and trapezoidal lifters because the torque required to lift sliding materials along an inclined face angle for triangular lifters is higher than for rectangular and trapezoidal lifters.

Parabolic and round lifters have curved contact face, which enable particles to slide back when the lifter reaches at the shoulder position. The lifting action of their face requires high torque, which result to an increase in power consumption.

4.2.2 Effect of Lifter Profile on Impact Load

Figure 4.2, illustrates the effect of lifter profile on impact loading of balls. The simulations were conducted using 4 lifters, 40 % of mill filling and rotating at 75% of critical speed.

The lifter profiles marginally affect the amount of the impact loads inside the mill. The impact load reduces slightly with the increase of face angle when flat contact surface are used. Using rectangular lifters, a great number of balls and materials reach the toe position. This is due to the fact that contact face of the lifter, materials are lifted higher and hit the toe position with high impact energy which results in high impact load. When trapezoidal and triangular lifters were used, some materials early fall before reaching the toe position, and their impact force is less.

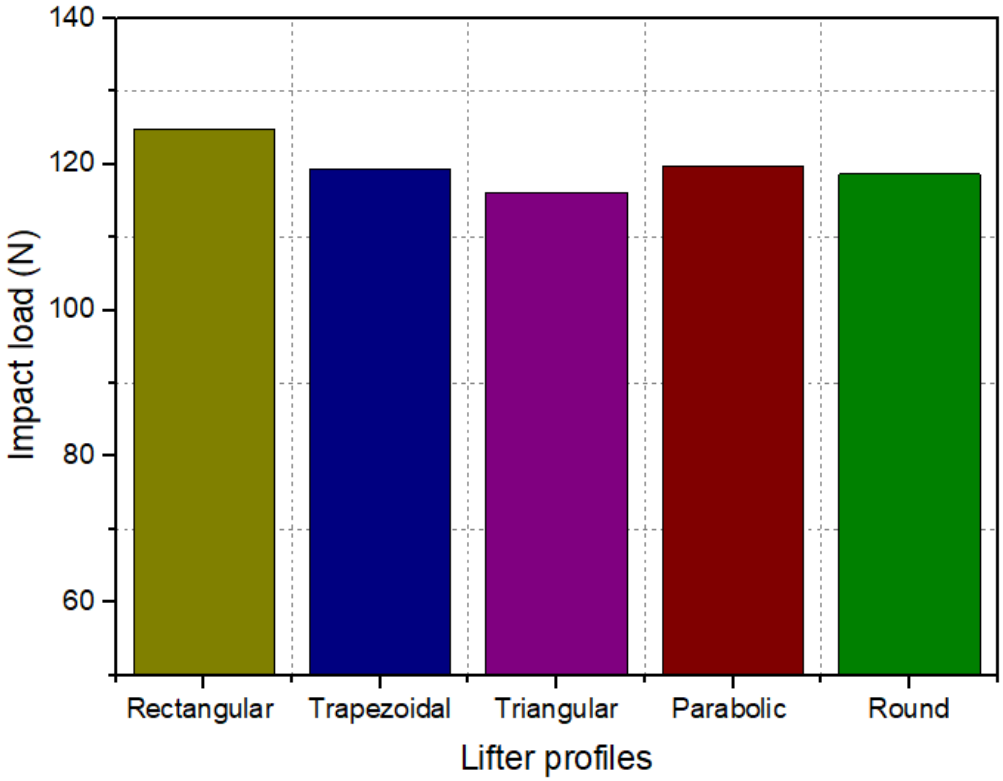

Figure 4.2: Impact load for ball mill with different lifter profile

When parabolic and round lifters were used, parabolic lifter showed high impact load than round lifters. This is due to the higher steep slope of parabolic face compared to round face. The steep slope allows grinding balls and materials to be lifted higher and fall with greater impact force at the toe. However, curved face lifters easily release materials to prematurely fall back before arrive at the toe position. Hence their lower impact load compared to flat contact faces. The same observation was reported by Datta (Datta et al., 1999) who reported that the face angle has an effect on the kinetic energy of balls inside the drum.

4.3 Effect of Number of Lifters

4.3.1 Effect of Number of Lifters on Power Consumption

Figure 4.3, depicts the variation of mill power with number of lifters. In this section, the mill filling level $J = 40\%$, $\phi = 75\%$, height of lifters H=20 mm, and the lifter number was changed from 2 to 12 lifters with an increment of 1.

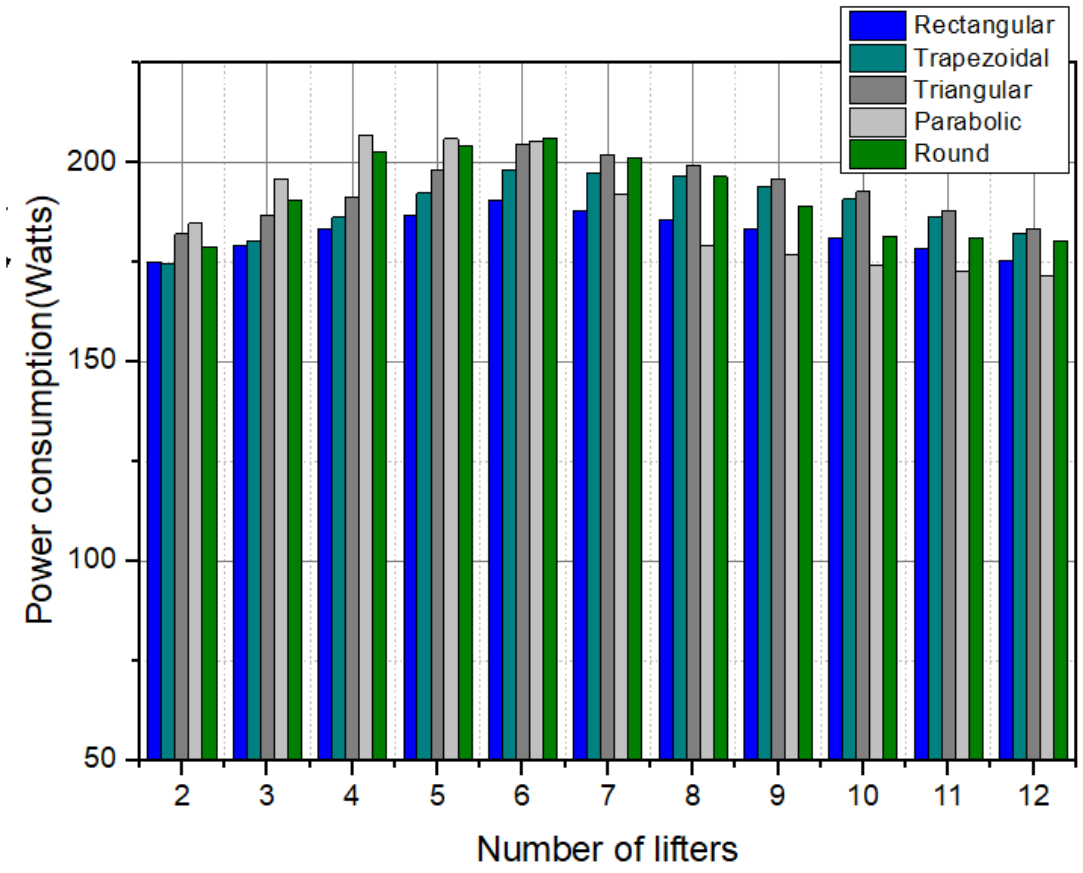

Figure 4.3: Variation of mill power with number of lifters

Lifting action and power consumption of a ball mill marginally depend upon the number of lifters. When the lifters are closely spaced; increased number of lifters, balls will be lifted to a greater height. When the number of lifter are 2 the number of particles lifted by two lifters is low, which resulted to lower power consumption. As the number of lifters increases, the cataracting motion of lifters also increased and the power draw increases. Beyond six lifters, the gap space between two lifters decrease so much such that two consecutive lifters lock-up the balls between them and the power consumption decreased. This observation corresponds to the results obtained by (Datta et al., 1999)

who observed that the increase of lifter number increases the power consumption, beyond a certain number of lifters; depending upon other factors, the power draw decreases. The same trend was reported by (Bian et al., 2017).

It was found that, at 2 lifters, the maximum power consumption was with parabolic lifter, followed by triangular lifter then round lifters. This is due to particle streams lifted from shoulder to toe position. From 3 to 6 lifters, curved contact face lifters drew more power than flat contact face lifters. This can be attributed to the increased number of sliding materials before reaching the toe when curved contact face are used. From 6 to 8 lifters, the volume of drum start to reduce due to the increased number of lifters which also decreased the cataracting materials. Therefore high energy is required to lift the materials. Beyond 6 lifters the power consumption decreased with the increase in number of lifters. Rectangular, trapezoidal and triangular lifters drew maximum power at 6 lifters. The number of lifters that consumed maximum power consumption for parabolic and round lifters were 4 to 6 lifters. Figure 4.3, shows that, in general the increase of lifters from 0 to 6 slightly increased the power draw, then decreases when lifter number is increased further from 6 to 12.

4.3.2 Effect of Number of Lifters on Impact Load

Figure 4.4 shows that increasing the number of lifters from 2 to 4, the impact load of mill with rectangular lifters was maximum followed by trapezoidal lifters and then came triangular lifters. Trapezoidal and triangular lifters have steep face angle, the lifting action of these faces to the cataracting motion is less than with rectangular lifters.

Parabolic and round lifters also have a marginally less impact load due to the sparse release of particles. When the lifter number was increased further from 6 to 10, the lifting action increased further. The impact load of trapezoidal and triangular lifters surpassed the rectangular lifters. This is due to the reduction of space between two successive lifters, therefore number of collision at the toe increased. A great number of materials is locked up for rectangular lifters followed by trapezoidal then comes triangle. When number of lifters is increased further from 10 to 12, the overall impact load reduced due to locked up materials that prevent particles to hit at the toe. Similar trends was reported in the literature by Djordjevic and Rezaeizadeh (Rezaeizadeh, Fooladi, Powell, & Mansouri, 2010; Djordjevic et al., 2004).

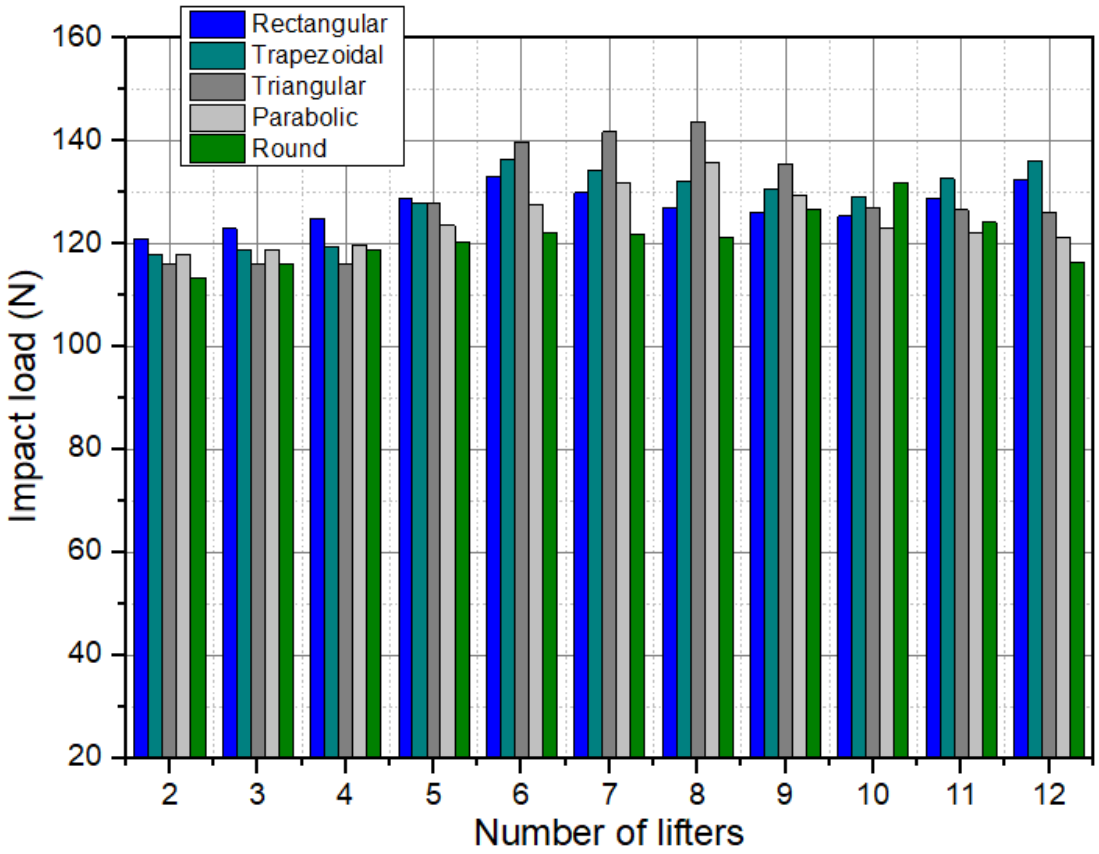

Figure 4.4: Variation of impact load with lifter number for flat lifters

4.4 Effect of Lifter Height

Lifter height is another parameter that was considered when analyzing the power consumption of small scale ball mills. Rectangular, trapezoidal, and triangular lifters were used. Parabolic and round lifters were not considered in subsequent analysis. This is due to the observation (shown in Figures 4.1, 4.2, 4.3, and 4.4 respectively) that parabolic and round lifters drew more power and lower impact load.

4.4.1 Effect of Lifter Height on Power Consumption

The effects of lifter height were investigated when the mill is loaded at 40% of mill volume. The variation of power consumption with respect to the lifter height is shown in Figure 4.5. Four lifter height (H) have been considered, (H=0 mm, H=10 mm, H=20 mm, and H=30mm). A drum of 4 lifters has been used in this study, rotating at mill speed of 75% of critical speed.

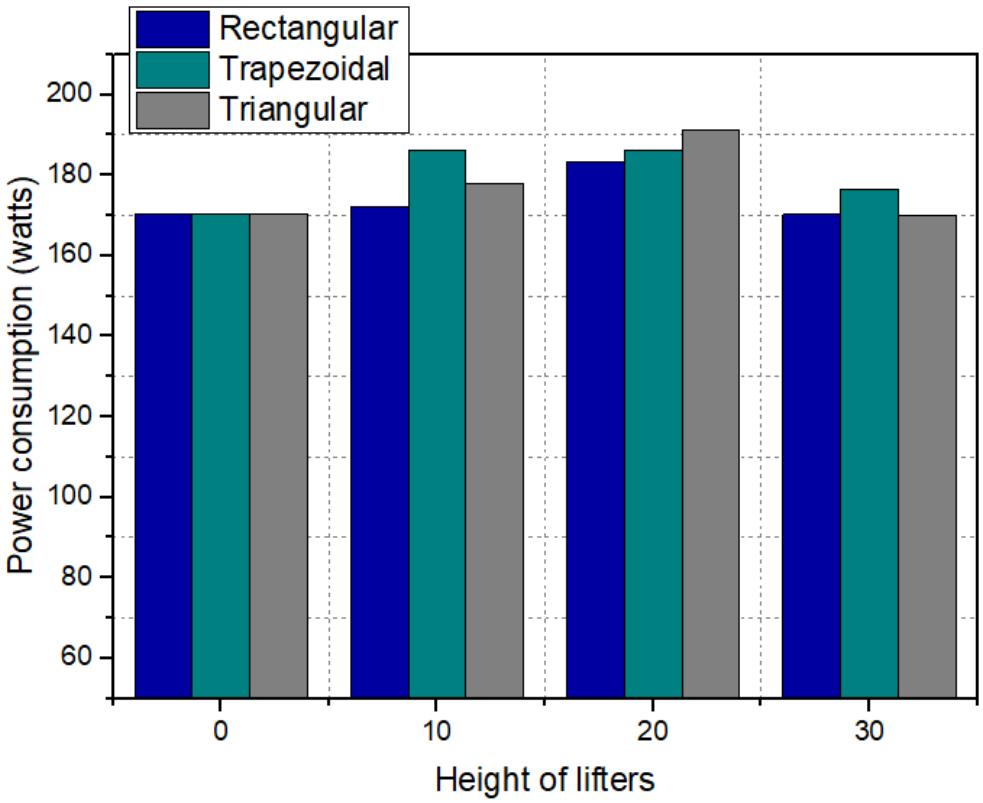

Figure 4.5: Variation of mill power with lifter height

The results showed that, when height H=0 mm is used, the power consumption was low. The Particles could not be lifted high, rather they moved slipping along the drum wall. At H=10, the power consumption slightly increased. Trapezoidal lifters drew more power compared to rectangular and triangular lifters. At H=20 mm, the maximum power consumption was when triangular lifters are used. At H=30 mm, the power consumption reduced. It can be noted that, when the lifter height is increased, the balls and materials will be lifted higher and increase the velocity of fall. This will cause the mill power to also increase but after a certain height, the effective volume of mill reduce which resulted in reduction of ball motion and thus; mill power decreased. This agrees with the literature published by (Datta et al., 1999; Bian et al., 2017; Usman, Taylor, & Spiller, 2017; Rezaeizadeh et al., 2010) who reported that the lifter height increases with the increase in mill power to the point that mill power passes through a peak as the lifter number increases, thereafter the power draw decreases.

4.4.2 Effect of Lifter Height on Impact Load

Figure 4.6, shows the variation of impact load with the change of lifter height at the mill speed of 75%. Increasing the lifter height lifts the grinding balls to an increased height and results in higher impact velocity.

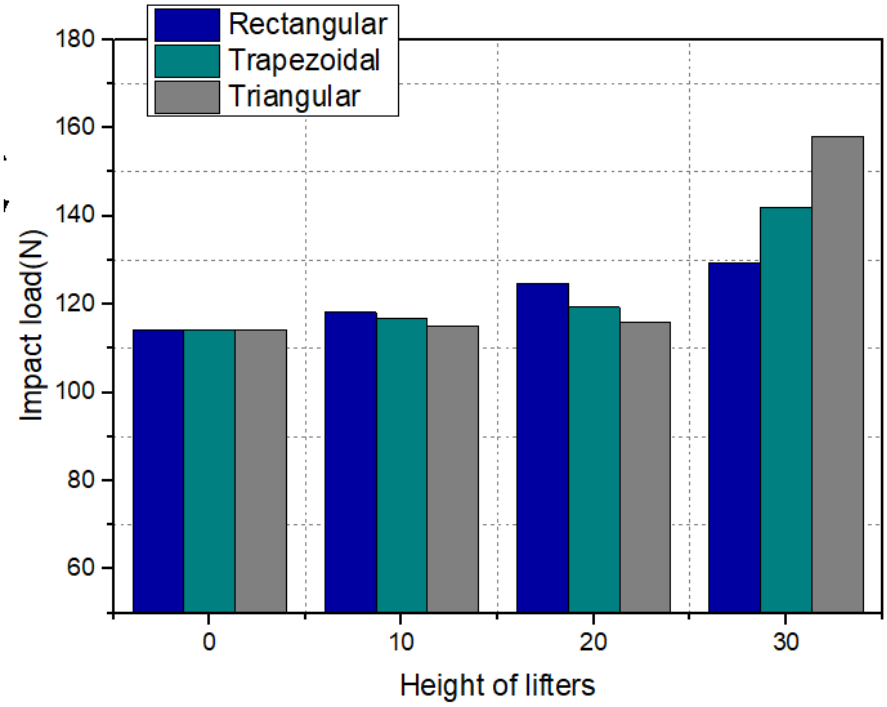

Figure 4.6: Variation of impact load with lifter height

It is observed that increasing the lifter height from 0 to 20 mm, the impact load slightly increased with the increase of number of lifters. Increasing the height of lifters also increased the lifting action of grinding balls higher and leads to the increase in impact load. At 30 mm of lifter height, the impact load increased further.

Rectangular lifters showed higher effect on impact load when a height of 10 mm and 20 mm are used. The reason is that, when the lifter height is still low, the lifting action is determined by face angle, whereas at 30 mm of lifter height, the impact load depends on the number of particles hit the toe position. Trapezoidal and triangular lifters showed lowe impact load at 10 and 20 mm of height. This is due to their face which when the lifter height is increased, the particles will fall back before reaching the toe. By increasing the lifter height from $0-30$ mm, the impact load increased with an average deviation of 5.5 N for rectangular lifters, with an average deviation of 9.5 N for trapezoidal lifters, and with

an average deviation of 16.1 N for triangular. Similar trend was observed in the literature (Rezaeizadeh et al., 2010; Yin et al., 2017) who reported that increasing the height of the lifters will enables them to raise up the larger particles to a greater height, and therefore result in higher impacts loads.

4.5 Effect of Mill Speed

4.5.1 Effect of Mill Speed on Power Consumption

Figure 4.7, shows that the motion of balls becomes more cataracting as the mill speed increases which lead to the mill power increase. However, as the mill speed increases further towards the critical speed, a great number of balls start to stick to the mill wall, the effective ball mass reduces and thus, the power consumption decreases. In this context, it is noted that the increase of the power depends upon the motion of the grinding media which also depends on the lifter profile that lifter up the balls. This observation agrees with the literature (Francioli, 2015; Yin et al., 2017; Datta et al., 1999)

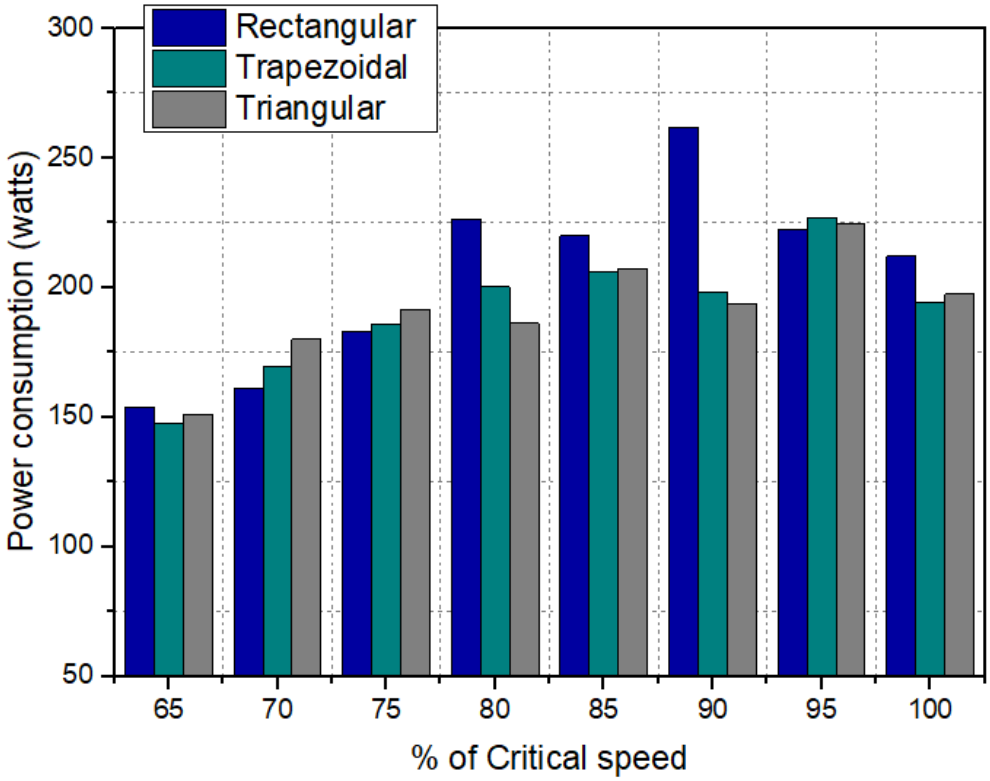

Figure 4.7: Variation of mill power with % of critical speed for flat lifters

It was observed that, the power consumption is maximum at an average speed of 90% of critical speed. When the ball mill is rotating at relatively low speed below 75% of the critical speed, the power consumption is relatively low. The reason is that particles have low kinetic energy. The power consumption starts decreasing at the speed is greater than 90%. Rectangular, compared to trapezoidal and triangular lifters drew less power at relatively low speed and highest power consumption at a speed greater than 75% of critical speed. This can be attributed to the early release of particles for trapezoidal and triangular lifters at low speed that requires higher torque to lift the materials, and when the speed is increased higher, the lifting action is determined by the centrifugal forces. This observation agrees with the results from the work of Hlungwani who observed that more balls are projected into the further cataracting region by the square lifters than by the trapezoidal lifters (Hlungwani et al., 2003).

4.5.2 Effect of Mill Speed on Impact Load

The mill speed has significant effect on impact load inside the mill. Figure 4.8 shows the effect of mill speed on the value of impact loads. It was observed that the impact load increases with the increase of the mill speed.

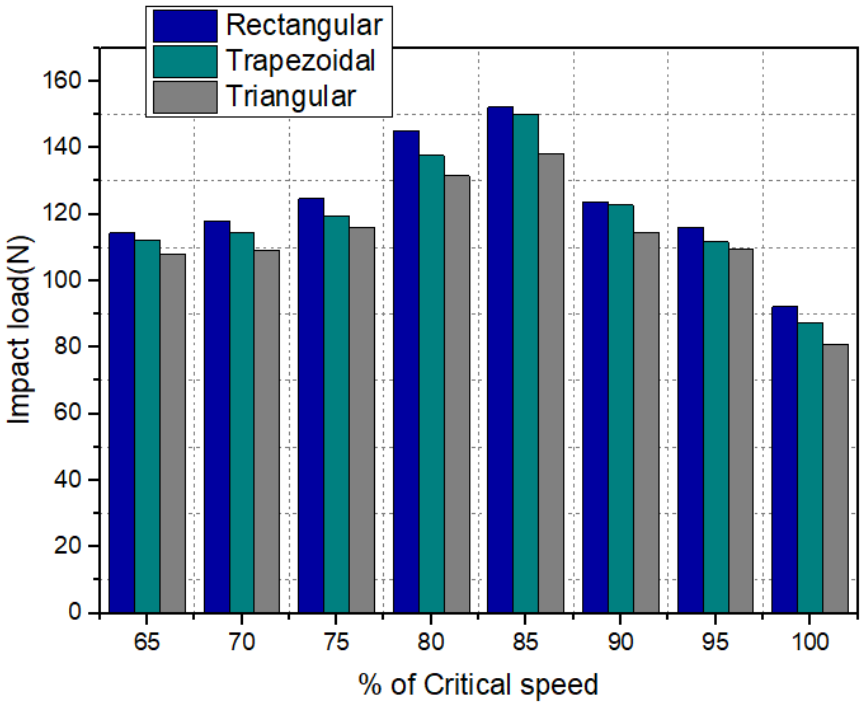

Figure 4.8: Variation in impact load with % critical speed for flat lifters

As the speed increases from 65% to 85% of critical speed, the maximum impact load increase with an average deviation of 14.17 N for rectangular lifters, with an average deviation of 13.66 N for trapezoidal, and an average deviation of 11.42 N for triangular lifters. It can be noted that the impact load for rectangular lifters is higher compared to trapezoidal and triangular lifters. When the speed was increased further, the impact load decreased. This was due to centrifugal motion of particles sticking to the wall of the drum, which reduced the impact energy. The same results have been reported by (Rezaeizadeh et al., 2010; Yin et al., 2017) in the literature who observed that beyond 75% of critical speed, the impact energy decreases significantly.

4.6 Sieve Analysis of Basalt Materials

The analysis of size distribution of Basalt materials were conducted, to validate the impact of rotating speed on the throughput size. This analysis was done by analyzing samples taken after discharging materials from the drum of the ball mill. 200g was taken as sample for all range of critical speed used in experiments.

Figure 4.9, illustrates a comparison of basalt size distribution for the mill rotating at 65 – 85% of critical speed(Cr), 40 % of mill filling charge, and 4 rectangular lifters as it is tabulated in Appendix IV.

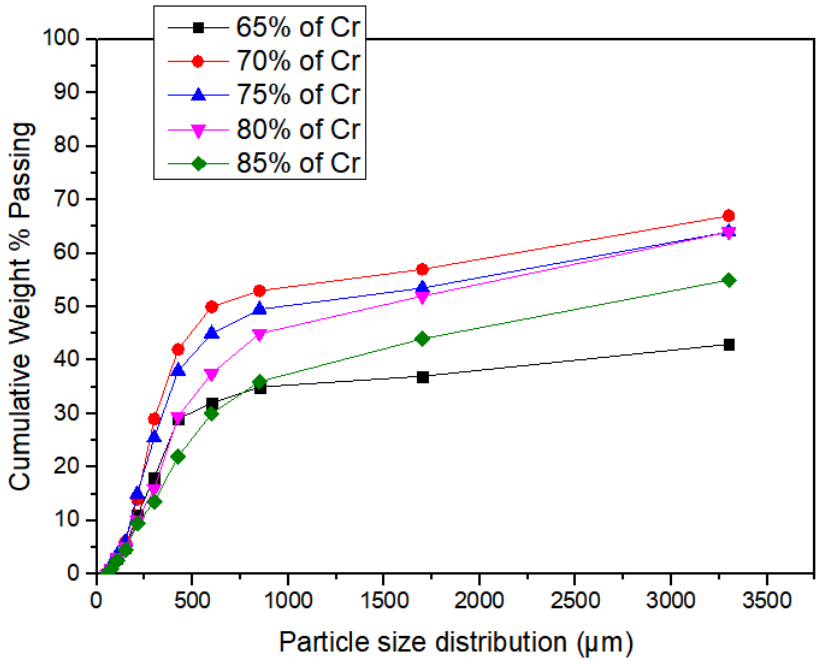

Figure 4.9: Cumulative size distribution graph for different mill speed

It was observed that the size distributions for 70, 75, and 80% of critical speed have finer grades of basalt. It can be noted that at 70% of critical speed, the overall performance of the small scale ball mill is high. This can be attributed to the high impact load at 70, 75, and 80% of the critical speed. This observation agrees with the work of (Usman et al., 2017; Francioli, 2015) respectively.

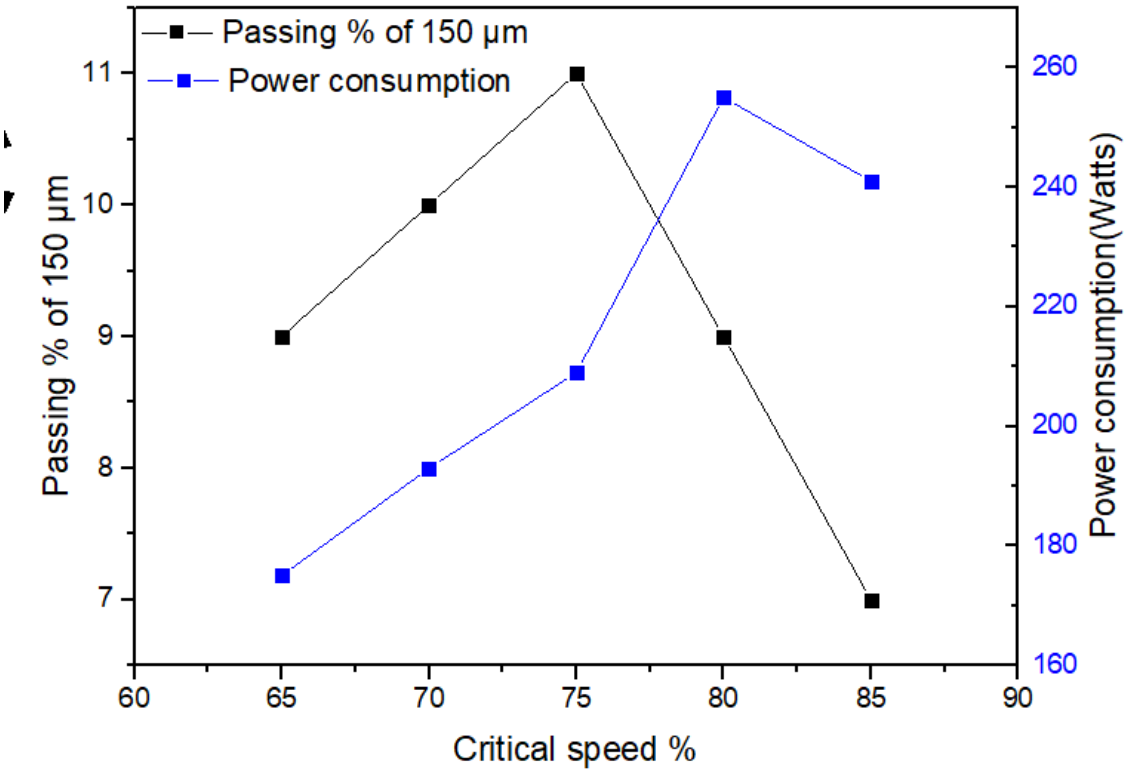

Figure 4.10: Comparison of power consumed and passing materials

It can be observed in Figure 4.10 and Table 4.1, that the mill rotating at 75% of critical speed has higher percentage of passing materials in a sieve of 150 μm and low power consumption.

Table 4.1: Comparison of power consumed and passing materials

% of Critical Speed	% of 150μm passing	Power (Watts)
65	9	175
70	10	193
75	11	209
80	9	255
85	7	241

This implies that, the small scale ball mill built in JKUAT can produce finer basalt material rotating at 75% of the critical speed. The power consumption of the ball mill at 80 and 85% was higher due to high cataracting motion of balls with lower percentage of finer materials because the balls are not hitting the toe position.

CHAPTER FIVE
CONCLUSIONS AND RECOMMENDATIONS

5.1 Conclusions

In this study 3D DEM modeling was used to study the effect of lifter geometry on the power consumption as well as on impact load for small scale batch grinding mills. This is important to optimize the grinding process and also to know the speed at which ball mill with different lifter profile can use for effective performance. In brief, the following conclusions can be drawn from the DEM simulations and experimental analysis of the effect of lifter configuration and mill speed on power consumption and impact load of a small scale ball mill:

- It has been observed that the change in lifter profile significantly affect the power consumption and impact load. This can be attributed to the change in contact face angle which when it is increased from $0 - 26.56$ degrees, the power consumption increased with an average deviation of 8.53 watts. It was concluded that rectangular, trapezoidal, and triangular lifters can effectively be used for small scale ball mill as they have higher impact load and lower power consumption at 75% of critical speed compared to parabolic and round lifters.

- It was concluded that, for rectangular lifters, a ball mill of 4 lifters of 30 mm height, at a rotating speed of 75% drew less power and have higher impact load and can be used for mineral processing on small scale. It was also concluded that, trapezoidal profile of 8 lifters and 30 mm height at a speed of 85% which showed higher impact load and less power consumption can provide better performance. Triangular lifter profile can provide better grinding results using (6-8) lifters of 30 mm height at 85% critical speed.

- Increasing lifter height marginally increased the power consumption. This draws to a conclusion that the lifter height of 30 mm can be used because it provides relatively low power consumption and higher impact load for rectangular, trapezoidal, and triangular lifter profiles.

- Mill speed has significant effect on the ball motion, impact load, and power consumption. It was concluded that, small scale ball mill can reach the best performance at the mill speed ranging from 75% to 85% of critical speed, That correspond to the

maximum percent of the impact load and lower power consumption.

- For the case study in Migori County, it was concluded that, the small scale ball mill of 4 rectangular lifters of 30 mm height at 75% of the critical speed and 40% of charge can provide higher finer throughput materials.

5.2 Recommendations for Future Work

From this research work, the effect of different lifter profiles provided substantial information that can be useful during the design and the use of small scale ball mill. While many parameters were evaluated, some limitations were observed and other parameters were considered to be beyond the scope of this research. However, the following recommendations were outlined for further study:

(a) In this study, five lifter profiles were investigated and their effect on the power consumption using one ore material, it is therefore recommended to study the grindability of other different materials and their effect on the power consumption of a ball mill.

(b) This study evaluated the effect of lifter profile on power consumption and impact load. However, it was observed in the conducted experiments that the lifter profile wears as the ball grinds for a long period of time. It is therefore recommended to investigate the effect of wearing of lifters and mill shell and their impact on the performance of a ball mill.

(c) In this study, a small cylindirical ball mill has been used to evaluate the power consumption and impact load. It is recommended to further investigate on the behavior of charge using other different mill designs such as hexagonal mills which are also applied by SMEs to provide a deeper comparison on the effective performance.

References

Austin, L. G., & Shoji, K. (1976). The Effect of Ball Size on Mill Performance. *Powder Technol.*, *19*, 71–79.

Balaz, P. (2008). High-Energy Milling. *Mechanochemistry Nanosci. Miner. Eng.*.

Bian, X., Wang, G., Wang, H., Wang, S., & Lv, W. (2017). Effect of lifters and mill speed on particle behaviour, torque, and power consumption of a tumbling ball mill: Experimental study and DEM simulation. *Miner. Eng.*, *105*, 22–35. Retrieved from `http://dx.doi.org/10.1016/j.mineng.2016.12.014` doi: 10.1016/j.mineng .2016.12.014

Bond, F. C. (1968). Crushing and grinding calculations, part. *Br. Chem. Eng.*.

Börner, M. (2011). *Discrete Elemente Method (DEM)* (Tech. Rep.).

Campbell, C. S., & Brennen, C. E. (1985). Computer simulations of granular shear flows. *J. Fluid Mech.*, *151*, 167–188.

Chandramohan, R., & Powell, M. S. (2005). Measurement of particle interaction properties for incorporation in the discrete element method simulation. *Miner. Eng.*, *18*(12), 1142–1151. doi: 10.1016/j.mineng.2005.06.004

Cleary, P. W. (2001). Charge behaviour and power consumption in ball mills: Sensitivity to mill operating conditions, liner geometry and charge composition. *Int. J. Miner. Process.*, *63*(2), 79–114. doi: 10.1016/S0301-7516(01)00037-0

Cleary, P. W., & Hoyer, D. (2000). comparison of DEM predictions with experiment. *Int. J. Miner. Process.*, 131–148.

Cleary, P. W., & Morrison, R. D. (2011a). Understanding fine ore breakage in a laboratory scale ball mill using DEM. *Miner. Eng.*, *24*(3-4), 352–366. Retrieved from http://dx.doi.org/10.1016/j.mineng.2010.12.013 doi: 10.1016/j.mineng.2010.12.013

Cleary, P. W., & Morrison, R. D. (2011b). Understanding fine ore breakage in a laboratory scale ball mill using DEM. *Miner. Eng.*, *24*(3-4), 352–366. Retrieved from http://dx.doi.org/10.1016/j.mineng.2010.12.013 doi: 10.1016/j.mineng.2010.12.013

Corporation, F. (n.d.). *Technical data Fluke 1735* (Tech. Rep.).

Cundall, P. A., & Strack, O. D. L. (1979). A discrete numerical model for granular assemblies. *Géotechnique*, *29*(1), 47–65. Retrieved from http://www.icevirtuallibrary.com/doi/10.1680/geot.1979.29.1.47 doi: 10.1680/geot.1979.29.1.47

Dahner, J., & Bosch, A. V. D. (2011). Total primary milling cost reduction by improved liner design. *J. South. African Inst. Min. Metall.*, *111*(October 2010), 11–14.

Daniel, S., & Tadeusz, T. (2010). Aspects of comminution flowsheets design in processing of mineral raw materials. *Gospod. Surowcami Miner. / Miner. Resour. Manag.*.

Dantu, P. (1957). Contribution a l'etude mecanique et geometrique des milieux pulverulents. In *Proc. 4th icsmfe, london.*

Datta, A., Mishra, B. K., & Rajamani, R. K. (1999). Analysis of power draw in ball mills by the discrete element method. *Can. Metall. Q.*, *38*(2), 133–140. doi: 10.1016/

S0008-4433(98)00039-1

de Carvalho, R. M. (2013). *Mechanistic modelling of semi-autogenous grinding* (Unpublished doctoral dissertation). Universidade Federal do Rio de Janeiro.

DEM Solutions. (2011). *EDEM 2.4 User Guide.*

Deniz, V. (2004). The effect of mill speed on kinetic breakage parameters of clinker and limestone. *Cem. Concr. Res.*, *34*, 1365–1371. doi: 10.1016/j.cemconres.2003.12.025

Djordjevic, N., Shi, F. N., & Morrison, R. (2004). Determination of lifter design, speed and filling effects in AG mills by 3D DEM. *Miner. Eng.*, *17*(11-12), 1135–1142. doi: 10.1016/j.mineng.2004.06.033

Ene, G. (2007). The Grinding Charge of Rotary Mills. *Ann. "Dunarea Jos" Univ. Galati*, 35–41.

Francioli, D. M. (2015). *Effect of operational variables on ball milling* (Unpublished doctoral dissertation).

Fuerstenau, D. W., & Lutch, J. J. (1999). The effect of ball size on the energy efficiency of hybrid high-pressure roll mill r ball mill grinding. *Powder Technol.*, 199–204.

Ghaboussi, J., & Barbosa, R. (1990). Three-dimensional discrete element method for granular materials. *Int. J. Numer. Anal. Meth. Geomech.*, *14*(7), 451–472. doi: 10.1002/nag.1610140702

Gupta, V., Zouit, H., & Hodouin, D. (1985). The Effect of Ball and Mill Diameters on Grinding Rate Parameters in Dry Grinding Operation. , *42*(August 1982), 199–208.

Gupta, V. K., & Sharma, S. (2014). Analysis of ball mill grinding operation using mill power specific kinetic parameters. *Adv. Powder Technol.*, *25*(2), 625–634. Retrieved from http://dx.doi.org/10.1016/j.apt.2013.10.003 doi: 10.1016/j.apt.2013.10.003

Härtl, J., & Ooi, J. Y. (2008). Experiments and simulations of direct shear tests: Porosity, contact friction and bulk friction. *Granul. Matter*, *10*(4), 263–271. doi: 10.1007/s10035-008-0085-3

Hlungwani, O., Rikhotso, J., Dong, H., & Moys, M. H. (2003). Further validation of DEM modeling of milling: Effects of liner profile and mill speed. *Miner. Eng.*, *16*(10), 993–998. doi: 10.1016/j.mineng.2003.07.003

Ipek, H. (2007). Effect of grinding media shapes on breakage parameters. *Part. Part. Syst. Charact.*, *24*(3), 229–235. doi: 10.1002/ppsc.200601095

Jaeger, J. (2005). *New solutions in contact mechanics*. WIT Press. Retrieved from https://books.google.co.ke/books?id=gpxRAAAAMAAJ

Jankovic, A., Dundar, H., & Mehta, R. (2010). Relationships between comminution energy and product size for a magnetite ore. (June 2008), 17–20.

John M.Ting, B. T. (1988). Strength behavior of granular materials using discrete numerical modelling. In *6th int. conf. numer. methods geomech.*

Johnson, K. L. (1985). Normal contact of elastic solids – Hertz theory. In *Contact mech.* (pp. 84–106). Cambridge University Press. doi: 10.1017/CBO9781139171731.005

Kabezya, & Motjotji, H. (2015). The Effect of Ball Size Diameter on Milling Perfor-

mance. *J. Mater. Sci. Eng.*, *4*(1), 4–6. doi: 10.4172/2169-0022.1000149

Kanda, Y., Simodaira, K., Kotake, N., & Abe, Y. (1999). Experimental study on the grinding rate constant of a ball mill: Effects of feed size and ball diameter. *KONA Powder Part. J.*, *17*(May), 220–226. doi: 10.14356/kona.1999030

Karunatilake, N., Kuhn, P., & Seibold, B. (2000). Dynamics of Balls and Liquid in a Ball mill. *Model. Semin. summer 2000*.

Kiangi, K. K., & Moys, M. H. (2008). Particle filling and size effects on the ball load behaviour and power in a dry pilot mill: Experimental study. *Powder Technol.*, *187*(1), 79–87. doi: 10.1016/j.powtec.2008.01.015

Kim, S., & Choi, W. S. (2008). Analysis of ball movement for research of grinding mechanism of a stirred ball mill with 3D discrete element method. *Korean J. Chem. Eng.*, *25*(3), 585–592. Retrieved from `http://dx.doi.org/10.1007/s11814-008-0099-x` doi: 10.1007/s11814-008-0099-x

King, R. P. (2000). *Technical Notes for Grinding*.

Kobayashi, M. K. M. N. T. (2007). Design Method of Ball Mill by Discrete Element Method. *Process Prod. Technol. Cent.*, 1–9.

Kohta, A., Hirotoshi, E., & Etsuo, A. (2009). Synthesis of HCP , FCC and BCC structure alloys in the Mg – Ti binary system by means of ball milling. *J. Alloys Compd.*(July). doi: 10.1016/j.jallcom.2009.01.086

Kulya, C. (2008). *Using Discrete Element Modelling (DEM) and Breakage Experiments To Model The Comminution Action in a Tumbling Mill* (Master thesis). University

of Cape Town.

Kyalo, M. N., Ndiritu, H., & Mwangi, D. (2017). *RPE Project progress Report II Improving comminution for Artisanal and Small scale Gold Miners in Kenya* (Tech. Rep.). Research,Production and Extension (RPE) JKUAT.

Lorig, L. J., Brady, B. H. G., & Cundall, P. A. (1986). Hybrid Distinct Element Boundary Element Analysis of Jointed Rock. *Int. J. Rock Mech. Min. Sci.*, *23*(4), 303–312. doi: Doi10.1016/0148-9062(86)90642-X

Lynch, A. J., & Rowland, C. A. (2015). *The History of Grinding*.

Magdalinovic, N., Trumic, M., & Andric, L. (2012). The optimal ball diameter in a mill. *Physicochem. Probl. Miner. Process.*, *48*(2), 329–339. doi: 10.5277/ppmp120201

Makokha, A. B., & Moys, M. H. (2006). Towards optimising ball-milling capacity : Effect of lifter design. *Miner. Eng.*, *19*, 1439–1445. doi: 10.1016/j.mineng.2006.03.002

Makokha, A. B., Moys, M. H., & Bwalya, M. M. (2011). Modeling the RTD of an industrial overflow ball mill as a function of load volume and slurry concentration. *Miner. Eng.*, *24*(3-4), 335–340. Retrieved from `http://dx.doi.org/10.1016/j.mineng.2010.11.001` doi: 10.1016/j.mineng.2010.11.001

Makokha, A. B., Moys, M. H., Bwalya, M. M., & Kimera, K. (2007). A new approach to optimising the life and performance of worn liners in ball mills : Experimental study and DEM simulation. *Int. J. Miner. Process.*, *84*, 221–227. doi: 10.1016/j.minpro.2006.09.009

Michael, M. H. (1988). The effects of mill speed and filling on the behaviour of the load

in a rotary grinding mill *. *J . S. Afr . Inst. Min. Met.*, *88*(February), 49–57.

Mio, J. K. H., Saito, F., & Miyazaki, M. (2001). Correlation of grinding rate of gibbsite with impact energy in tumbling mill with mono-size balls. *Miner. Process. Extr. Metall.*, *14*(10), 1213–1223.

Mishra, B. K., & Rajamani, R. K. (1992). The discrete element method for the simulation of ball mills. *Appl. Math. Model.*, *16*(August 1991), 598–604.

Morrison, R. D., & Cleary, P. W. (2004). Using DEM to model ore breakage within a pilot scale SAG mill. *Miner. Eng.*, *17*(11-12), 1117–1124. doi: 10.1016/j.mineng .2004.06.016

Moys, M., Van nierop, M., Van Tonder, J., & Glover, G. (1998). Validatio of the discrete element method (DEM) by comparing predicted load behaviour of grinding mill with measured data. *Process Simul. Control*, 39–44.

M.Ting, J. (1992). A robust algorithm for ellipse-based discrete element modelling of granular materials. *Comput. Geotech. vol.*, *13*, 175–186.

Nadolski, S., Klein, B., Kumar, A., & Davaanyam, Z. (2014). An energy benchmarking model for mineral comminution. *Miner. Eng.*, *65*, 178–186. Retrieved from `http://dx.doi.org/10.1016/j.mineng.2014.05.026` doi: 10.1016/j.mineng.2014.05.026

Navarro, H. A., & de Souza Braun, M. P. (2013). Linear and Nonlinear Hertizian Contact Models for Materials in Multibody Dynamics. *22nd Int. Congr. Mech. Eng. (COBEM 2013)*, *2*(Cobem), 159–170.

Nistlaba, N., & Lameck, S. (2005). *Effects of Grinding Media Shapes on Ball Mill Performance* (Unpublished doctoral dissertation). University of the Witwatersrand,.

Peng, B. (2014). *Discrete Element Method (DEM) Contact Models Applied to Pavement Simulation* (Unpublished doctoral dissertation). the Virginia Polytechnic Institute and State University in.

Petrakis, E., Stamboliadis, E., & Komnitsas, K. (2017). Identification of Optimal Mill Operating Parameters during Grinding of Quartz with the Use of Population Balance Modeling †. *KONA Powder Part. J.*, *34*(34), 213–223. doi: 10.14356/kona.2017007

Powell, M. S., & Cleary, P. W. (2014). Selection and design of mill liners. *Adv. Comminution*(January 2006).

Powell, M. S., & Mcbride, A. T. (2004). A three-dimensional analysis of media motion and grinding regions in mills. *Miner. Eng.*, *17*, 1099–1109. doi: 10.1016/j.mineng .2004.06.022

Prasad, D. V., & Theuerkauf, J. (2010). Improvement in the collision intensity of grinding media in high energy impact mills. *Chem. Eng. Technol.*, *33*(9), 1433–1437. doi: 10.1002/ceat.200900392

R. Sarracino, A. McBride, & Powell, M. (2004). Using particle flow code to investigate energy dissipation in a rotary grinding mill. In *Numer. model. micromechanics via part. methods - 2004* ... (p. 111.).

Raasch, J. (1992). Trajectories and Impact Velocities of Grinding Bodies in Planetary Ball Mills. *Chem. Eng. Technol.*, *15*, 245–253.

Rezaeizadeh, M., Fooladi, M., Powell, M. S., & Mansouri, S. H. (2010). Experimental observations of lifter parameters and mill operation on power draw and liner impact loading. *Miner. Eng.*, *23*(15), 1182–1191. Retrieved from http://dx.doi.org/10.1016/j.mineng.2010.07.017 doi: 10.1016/j.mineng.2010.07.017

Rhodes, M. (2008). *Introduction to Particle Technology – Second Edition* (Second ed.; R. Martin, Ed.).

Rittinger, P. V. (1867). *Lehrbuch der aufbereitungskunde in ihrer neuesten entwicklung und ausbildung systematisch dargestellt*. Publisher Ernst & Korn (Gropius'sche buch- und kunsthandlung).

Rowland, C. A. (2006). Bond's method for selection of ball mills. *Adv. Comminution*, 385–397.

Royston, D. (2008). Semi-autogenous grinding (SAG) mill liner design and development. *Miner. Metall. Process.*, *24*(3), 121–132.

Sergio, M., Matos, V., Luiz, A., Mesquita, A., Mascarenhas, F. P., & Carlos, L. (2013). Study Of Influence Of Vibration Parameters On The Efficiency Of Horizontal Vibrating Screen Using The Discrete Element Method 2 . Discrete Element Method (Dem). In *Proc. xxxiv iber. latin-american congr. comput. methods eng. z.j.g.n del prado (editor), abmec, pirenópolis, go, brazil, novemb. 10-13, 2013.*

Soleymani, M., Fooladi, M., & Rezaeizadeh, M. (2017). Experimental study the impact forces of tumbling mills. *Proc. Inst. Mech. Eng. Part E J. Process Mech. Eng.*, *231*(2), 1–11. doi: 10.1177/0954408915594526

Sullivan, C. O. (2008). Particle-Based Discrete Element Modelling : A Geomechanics Overview. In *12th int. conf. int. assoc. comput. methods adv. geomech.* (pp. 1–6).

Sun, Y. I., Dong, M., Mao, Y., & Fan, D. (2008). Analysis on Grinding media Motion in Ball Mill by Discrete Element Method. In *Proc. 1st int. conf. manuf. eng. qual. prod. syst. (volume i) anal.* (Vol. I, pp. 227–231).

Tanaka, T. (1966). Comminution laws. In *Ind. eng. chem. process des. dev. vol. 1-4* (Vol. 5, pp. 353–358). American Chemical Society, 1962.

Tang, P., & Puri, V. M. (2004). Methods for minimizing segregation: A review. *Part. Sci. Technol.*, *22*(4), 321–337. doi: 10.1080/02726350490501420

U.S Department of energy. (2007). *Mining Industry Energy Bandwidth* (Tech. Rep.).

Usman, H. (2015). *Measuring the Efficiency of the Tumbling Mill As a Function of lifter configuration and operating parameters* (Unpublished doctoral dissertation).

Usman, H., Taylor, P., & Spiller, D. E. (2017). The effects of lifter configurations and mill speeds on the mill power draw and performance. *AIP Conf. Proc.*, *1805*. doi: 10.1063/1.4974432

Van Nierop, M. A., Glover, G., Hinde, A. L., & Moys, M. H. (2001). A discrete element method investigation of the charge motion and power draw of an experimental two-dimensional mill. *Int. J. Miner. Process.*, *61*(2), 77–92. doi: 10.1016/S0301-7516(00)00028-4

Wills, B. (1993). Grinding mills. In T. Napier-Munn (Ed.), *Will's miner. process. technol.* (Seventh ed., pp. 146–160). doi: 10.1016/B978-0-08-034937-4.50016-8

Wills, B. A., & Napier-munn, T. (2006). *Preface to 7th Edition, Mineral Processing Technology* (7th ed.) (No. October). Elsevier Science & Technology Books.

World Health organization. (2016). *Artisanal and small-scale gold mining and health* (Tech. Rep.).

Yin, Z., Peng, Y., Zhu, Z., Yu, Z., & Li, T. (2017). Impact load behavior between different charge and lifter in a laboratory-scale mill. *Materials (Basel).*, *10*(8). doi: 10.3390/ma10080882

APPENDICES

Appendix I: Small Scale Ball Mill Design Built in JKUAT

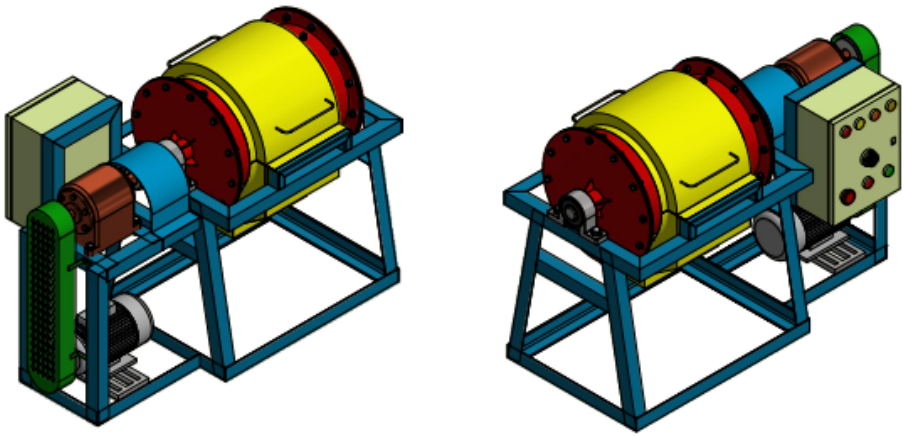

Figure I.1: Small scale ball mill design buit in JKUAT

Figure I.1 illustrates the designed small scale ball mill in JKUAT. It comprises of a cylindrical drum supported by a supporting frame, power transmission and speed control box.

Appendix II: Exploded View of the Small Scale Ball Mill Assembly

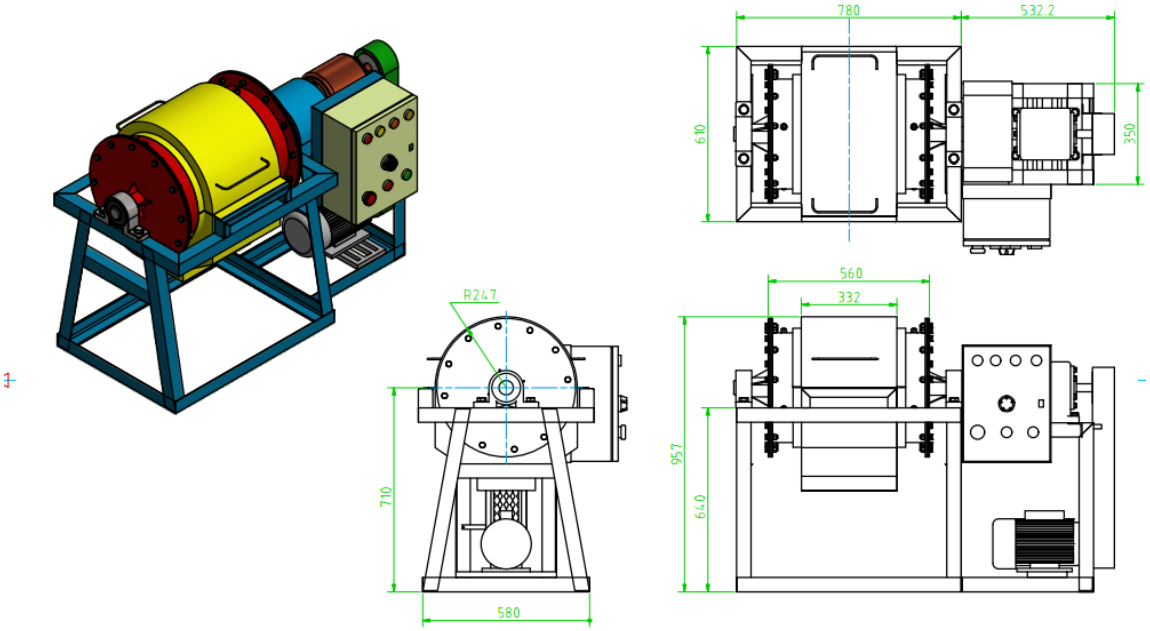

Figure II.1: Exploded View of the Small scale ball mill Assembly

Figure II.1, shows the exploded views of the small scale ball mill assembly.

Appendix III: Dimensions of Lifter Profile and their Face Angles

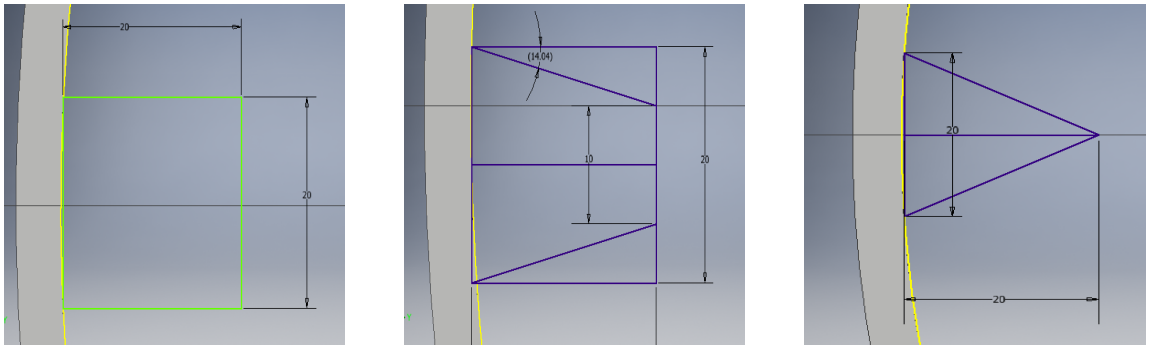

(a) Rectangular (b) Trapezoidal (c) Triangular

Figure III.1: Polygonal lifters with 20 mm width and 20 mm height

(a) Parabolic (b) Round

Figure III.2: Curved face lifters with 20 mm width and 20 mm height

Appendix IV: Sieving Analysis Table

Table IV.1: Sieving analysis using 200 grams sample of a Basalt material

N	Size (mm)	Sieve Weight (g)	Weight of sieve + ore at				
			65%	**70%**	**75%**	**80%**	**85%**
1	**3300**μm	416	498	482	488	488	498
2	**1700**μm	356	370	376	376	380	370
3	**850**μm	318	324	326	326	332	324
4	**600**μm	304	306	310	310	318	306
5	**425**μm	280	282	298	294	296	282
6	**300**μm	268	296	294	292	294	296
7	**212**μm	254	276	284	274	266	276
8	**150**μm	242	268	258	260	252	268
9	**106**μm	240	250	246	244	244	252
10	**75**μm	234	238	238	238	238	238
11	**53**μm	230	232	232	232	232	232
12	**pan**	298	298	298	298	298	298

Sieving analysis using 200 grams sample of a Basalt material for size distribution for different mill speed, 40% charge, 4 rectangular lifter profile